



HAL
open science

A meso-macro finite element modelling of laminate structures - Part II: Time-dependent behaviour

Mohamed Lamine Boubakar, Long Vang, Frédérique Trivaudey, Dominique Perreux

► **To cite this version:**

Mohamed Lamine Boubakar, Long Vang, Frédérique Trivaudey, Dominique Perreux. A meso-macro finite element modelling of laminate structures - Part II: Time-dependent behaviour. *Composite Structures*, 2003, 60(3) (3), pp. 275-305. 10.1016/S0263-8223(03)00012-6 . hal-00014073

HAL Id: hal-00014073

<https://hal.science/hal-00014073>

Submitted on 9 Jan 2024

HAL is a multi-disciplinary open access archive for the deposit and dissemination of scientific research documents, whether they are published or not. The documents may come from teaching and research institutions in France or abroad, or from public or private research centers.

L'archive ouverte pluridisciplinaire **HAL**, est destinée au dépôt et à la diffusion de documents scientifiques de niveau recherche, publiés ou non, émanant des établissements d'enseignement et de recherche français ou étrangers, des laboratoires publics ou privés.

A meso–macro finite element modelling of laminate structures

Part II: time-dependent behaviour

M.L. Boubakar*, L. Vang, F. Trivaudey, D. Perreux

Laboratoire de Mécanique Appliquée Raymond Chaleat, UMR-CNRS 6604, Université de Franche-Comté,
24 Chemin de l'Epitaphe, 25000 Besançon, France

A meso–macro modelling is proposed for laminates made of unidirectional layers of a polymer matrix reinforced with long fibres. The time-independent behaviour introduced in the first part of this article is improved herein to account for viscous phenomena through viscoelasticity and viscoplasticity. A spectrum-type viscoelastic model is considered, which is based on the definition of elementary viscoelastic mechanisms. Its mathematical formulation is simplified by using a relaxation times triangular layout. A generalised Norton-type model integrating the elastic domain concept is used to report the plastic strains delay. A zero-valued “dynamic” yield function is incorporated into the traditional viscoplastic format, allowing a same treatment of plastic and viscoplastic problems. The integration of the layer behaviour through the thickness is obtained within a Kirchhoff shell finite element. The constitutive equations are integrated using two families of algorithms that generalise the well-known trapezoidal and mid-point rules, for which accuracy and non-linear stability analysis are carried out. Significant robustness of the local iterative solution is provided by complementing the basic Newton’s scheme with a local line-search strategy. In the case of a fully coupled plastic–viscoplastic behaviour, the local Newton’s iterative scheme is associated with a grid-search method in order to define available initial solutions. A perturbation technique is suggested to evaluate an algorithmic tangent operator since the viscoelasticity renders non-trivial an explicit determination of a consistent tangent operator. The proposed formulation has been implemented in the finite element code CASTEM2000® in order to test its validity. The obtained results are compared with semi-analytical ones in the case of progressive repeated loading tests by applying pure traction and pure pressure. Creep tests are also considered.

To avoid ill-posed boundary value problems and to take account of a time-dependent damage process, viscous regularisation of the time-independent damage model is finally introduced with a structure analogous to the Perzyna-type viscoplasticity.

Keywords: Viscoelasticity; Viscoplasticity; Trapezoidal rule; Mid-point rule; Accuracy; Non-linear stability; Grid-search method; Perturbation technique; Localisation; Visco-damage

1. Introduction

Within the context of a mesoscopic approach to model the non-linear behaviour of laminate composites, the behaviour of a simple ply is firstly modelled, then the laminate one is assessed by a structural analysis. In a first contribution [1], the complete theoretical formulation of a damaged elasto-plastic layer model has been presented and successfully integrated within a Kirchhoff shell finite element. This model is improved by the present work to account for viscous phenomena through viscoelasticity and viscoplasticity.

A phenomenological approach with internal variables is chosen to describe the viscous properties of a layer. The behaviour constitutive equations are built into a thermodynamic framework with two potentials: the state potential or thermodynamic potential that gives the state laws and the dissipation potential that gives evolution laws for the internal variables through the generalised normality assumption. The Helmholtz free energy is chosen as thermodynamic potential and the Clausius–Duhem inequality is satisfied assuming that the viscoelastic and viscoplastic processes are independent.

* Corresponding author. Fax: +33-3-8166-6700.

E-mail address: lamine.boubakar@univ-fcomte.fr (M.L. Boubakar).

A spectrum-type viscoelastic model based on the definition of elementary viscoelastic mechanisms is adopted. Its formulation is simplified by choosing a relaxation times triangular layout. A generalised Norton-type viscoplastic model integrating the elastic domain concept is used to report the plastic strains delay. The viscoplasticity is interpreted herein as a penalty regularisation of the classical time-independent plasticity and a zero-valued “dynamic” yield function depending upon the adopted constitutive model is incorporated into its traditional format. The solution of a viscoplastic constitutive problem can then be issued by following the same reasoning used for time-independent models. (Under persistent viscoplastic flow, a consistency condition can be derived from the “dynamic” yield condition.)

For the building of an accurate and reliable state computation algorithm, the important problem in non-linear material analysis concerns the temporal integration of constitutive equations in the standard strain driven format. Hence, for example, in order to guarantee the numerical solution convergence towards the exact one as the step size tends to zero, any proposed algorithm should be consistent with the integrated constitutive equations and numerically stable. In this study, two families of algorithms that generalise the well-known trapezoidal and mid-point rules are considered, for which accuracy and non-linear stability (stability with respect to arbitrary perturbation in the initial conditions) analysis are carried out. A line-search strategy is adopted to determine the ensuing local iterative solutions. These solutions are obtained by enforcing the “dynamic” yield condition at different times depending upon the considered algorithm.

For a complete damaged elasto-dissipative modelling including time-dependent and time-independent effects, the state of the material is obtained over two steps: A (visco)elastic prediction–(visco)plastic correction, then a (visco)elasto-(visco)plastic prediction-damage correction. In the case of a fully coupled plastic–viscoplastic behaviour, the local Newton’s iterative scheme is associated with a grid-search method in order to define available initial solutions. A perturbation technique is suggested to evaluate an algorithmic tangent operator since the viscoelasticity renders non-trivial an explicit determination of a consistent tangent operator.

The so constructed numerical model has been implemented in the finite element code CASTEM2000® in order to test its validity. The obtained results are compared with semi-analytical ones in the case of progressive repeated loading tests by applying pure traction and pure internal pressure on a $[+55, -55]_6$ laminate tube. Creep tests are also considered.

To prevent localisation problems and to take account for a time-dependent damage process, a viscous regularisation of the time-independent damage model is finally introduced with a structure analogous to the Perzyna-type viscoplasticity. This regularisation produces retardation of micro-cracks growth and leads to well-posed boundary value problem. A relevant expression of the algorithmic tangent operator is proposed in this case. This is achieved by replacing the rate-independent damage consistency condition with a relation between the increment of the damage variable and the yield function of the constitutive model in use i.e. incremental “dynamic” yield condition for damage.

Tensors will be underlined in direct notation: $\underline{(\cdot)}$ represents a second order tensor and $\underline{\underline{(\cdot)}}$ a fourth order tensor. Their juxtaposition implies the usual summation operation. A superposed dot indicates the rate, superposed two dots indicate acceleration, a superposed -1 the inverse and a superposed T the transpose. \underline{I} and $\underline{\underline{I}}$ are, respectively, the second and the fourth order identity tensors. (In a Cartesian coordinates system $I_{ij} = \delta_{ij}$ and $I_{ijkl} = (1/2)(\delta_{ik}\delta_{jl} + \delta_{il}\delta_{jk})$).

2. Time-dependent behaviour of damaged composite layer

The viscous response of a damaged layer can be given in the absence of damage i.e. through an equivalent virgin layer, in terms of effective stresses $\hat{\underline{\sigma}}$ such as [1]:

$$\hat{\underline{\sigma}} = [\underline{I} + \underline{\underline{AH}}(D)]\underline{\sigma} \quad (1)$$

$\underline{\sigma}$ represents the Cauchy true stresses tensor, \underline{A} the elastic stiffness tensor and $\underline{\underline{H}}$ a perturbation tensor depending on the damage variable D which is assumed to be removed fictitiously in the effective stresses space.

2.1. Viscoelastic behaviour

Due to the relative displacement of unbroken molecular chains in the polymer matrix, reversible but time-dependent strains can be observed. Associated with a dissipative process, this kind of behaviour is classically described using the thermodynamics of irreversible processes [2–4].

Assuming that the state of the equivalent virgin material is completely defined by the elastic strains $\underline{\varepsilon}^e$ and a set of second order tensors $\underline{\xi}_i$ ($i \in N$) corresponding to viscoelastic flow elementary mechanisms, the Clausius–Duhem inequality gives the following state law and intrinsic dissipation In_{ve} :

$$\hat{\underline{\sigma}} = \rho \frac{\partial \hat{\psi}}{\partial \underline{\varepsilon}^e}, \quad \text{In}_{\text{ve}} = {}^T \underline{\varepsilon}^{\text{ve}} \hat{\underline{\sigma}} - \sum_i {}^T \underline{\xi}_i \dot{\underline{\chi}}_i \geq 0 \quad (2)$$

ρ being the material mass density and $\underline{\chi}_i = \rho \partial \hat{\psi} / \partial \underline{\xi}_i$ the thermodynamic forces associated with $\underline{\xi}_i$. $\underline{\varepsilon}^{\text{ve}}$ represents the viscoelastic strain rate tensor (in the absence of plastic flow, the total strains $\underline{\varepsilon}$ are composed of an elastic part $\underline{\varepsilon}^e$ and a viscoelastic part $\underline{\varepsilon}^{\text{ve}}$ depending on $\underline{\xi}_i$ i.e. $\underline{\varepsilon} = \underline{\varepsilon}^e + \underline{\varepsilon}^{\text{ve}}(\underline{\xi}_i)$).

In order to build a linear viscoelastic model, the following specific free energy $\hat{\psi}$ is introduced (no plastic flow):

$$\hat{\psi}(\underline{\varepsilon}^e, \underline{\xi}_i) = \frac{1}{2\rho} {}^T \underline{\varepsilon}^e \underline{\underline{A}} \underline{\varepsilon}^e + \frac{1}{2\rho} \sum_i \frac{1}{\mu_i} {}^T \underline{\xi}_i \underline{\underline{A}}_{\text{ve}} \underline{\xi}_i \quad (3)$$

With respect to a reference frame R_f having its first axis \bar{x}_1 along the fibres direction and its third one \bar{x}_3 following the thickness line, the elastic stiffness tensor is:

$$\underline{\underline{A}} = \begin{bmatrix} \frac{1}{E_1} & -\frac{\nu_{1l}}{E_1} & -\frac{\nu_{1t}}{E_1} & 0 & 0 & 0 \\ -\frac{\nu_{1l}}{E_1} & \frac{1}{E_t} & -\frac{\nu_{lt}}{E_t} & 0 & 0 & 0 \\ -\frac{\nu_{1l}}{E_1} & -\frac{\nu_{lt}}{E_t} & \frac{1}{E_t} & 0 & 0 & 0 \\ 0 & 0 & 0 & \frac{1}{G_{1t}} & 0 & 0 \\ 0 & 0 & 0 & 0 & \frac{1}{G_{1t}} & 0 \\ 0 & 0 & 0 & 0 & 0 & \frac{1}{G_{tt}} \end{bmatrix}^{-1}; \quad -\frac{\nu_{1l}}{E_t} = -\frac{\nu_{1t}}{E_1} \quad (4)$$

with E_1 (respectively E_t) the Young's modulus in the fibres direction (respectively in the transverse isotropic plane (\bar{x}_2, \bar{x}_3)), G_{1t} and G_{tt} the shear module in the planes (\bar{x}_1, \bar{x}_2) or (\bar{x}_1, \bar{x}_3) and in the plane (\bar{x}_2, \bar{x}_3) respectively and ν_{1t} , ν_{t1} and ν_{tt} the Poisson's ratios.

$\underline{\underline{A}}_{\text{ve}}$ is a fourth order tensor describing the viscous anisotropy and having the $\underline{\underline{A}}$ symmetries. Considering a pure elastic behaviour in the fibres direction, $\underline{\underline{A}}_{\text{ve}}$ is chosen as follows:

$$\underline{\underline{A}}_{\text{ve}} = \begin{bmatrix} 0 & 0 & 0 & 0 & 0 & 0 \\ 0 & \frac{\beta_t}{E_t} & -\beta_{tt} \frac{\nu_{tt}}{E_t} & 0 & 0 & 0 \\ 0 & -\beta_{tt} \frac{\nu_{tt}}{E_t} & \frac{\beta_t}{E_t} & 0 & 0 & 0 \\ 0 & 0 & 0 & \frac{\beta_{1t}}{G_{1t}} & 0 & 0 \\ 0 & 0 & 0 & 0 & \frac{\beta_{1t}}{G_{1t}} & 0 \\ 0 & 0 & 0 & 0 & 0 & \frac{\beta_{tt}^*}{G_{tt}} \end{bmatrix}^{-1}; \quad \frac{\beta_{tt}^*}{G_{tt}} = 2 \left(\frac{\beta_t}{E_t} + \beta_{tt} \frac{\nu_{tt}}{E_t} \right) \quad (5)$$

β_t , β_{tt} and β_{1t} are parameters characterising the material viscosity. The effect of each elementary viscous mechanism (i) is then differentiated using weighting coefficients μ_i .

From Eq. (3):

$$\underline{\chi}_i = \frac{1}{\mu_i} \underline{\underline{A}}_{\text{ve}} \underline{\xi}_i \quad (6)$$

According to a spectrum viscoelastic modelling [5,6], the viscoelastic strain rates are defined as a superposition of the elementary kinetics $\dot{\underline{\xi}}_i$:

$$\underline{\varepsilon}^{\text{ve}} = \sum_i \dot{\underline{\xi}}_i \quad (7)$$

what leads to the following form of the intrinsic dissipation:

$$\text{In}_{\text{ve}} = \sum_i {}^T \dot{\underline{\xi}}_i (\hat{\underline{\sigma}} - \underline{\chi}_i) \geq 0 \quad (8)$$

Each component (which corresponds to an elementary mechanism) being independent of the kinetics variables whose depend the other components, uncoupled dissipative processes can be defined:

$$(\text{In}_{\text{ve}})_1 = {}^T \dot{\underline{\xi}}_1 (\hat{\underline{\sigma}} - \underline{\chi}_1) \geq 0, \quad (\text{In}_{\text{ve}})_2 = {}^T \dot{\underline{\xi}}_2 (\hat{\underline{\sigma}} - \underline{\chi}_2) \geq 0, \quad (\text{In}_{\text{ve}})_i = {}^T \dot{\underline{\xi}}_i (\hat{\underline{\sigma}} - \underline{\chi}_i) \geq 0 \quad (9)$$

The driving forces $(\hat{\underline{\sigma}} - \underline{\chi}_i)$ are given by complementary laws.

Assuming normal dissipative processes [2,3], each $(\text{In}_{ve})_i$ can be expressed by a non-negative continuous convex function $\Pi_{ve}(\underline{\xi}_i)$, defined for all $\underline{\xi}_i$ and verifying $\Pi_{ve}(0_i) = 0$. In the particular case of positively homogeneous functions of order p , the complementary laws are then:

$$(\hat{\sigma} - \underline{\chi}_i) = \frac{1}{p} \frac{\partial \Pi_{ve}}{\partial \underline{\xi}_i} \quad (10)$$

The choice of the following quadratic functions ($p = 2$):

$$\Pi_{ve} = \frac{\tau_i}{\mu_i} (\Gamma \underline{\xi}_i \underline{A}_{ve} \underline{\xi}_i) \quad (11)$$

where τ_i are relaxation times, leads to:

$$(\hat{\sigma} - \underline{\chi}_i) = \frac{\tau_i}{\mu_i} \underline{A}_{ve} \underline{\xi}_i \quad (12)$$

Hence, taking account of Eqs. (6) and (7):

$$\underline{\xi}^{ve} = \sum_i \frac{1}{\tau_i} (\mu_i \underline{S}_{ve} \hat{\sigma} - \underline{\xi}_i); \quad \underline{S}_{ve} = \underline{A}_{ve}^{-1} \quad (13)$$

τ_i and μ_i are obtained from a relaxation times spectrum layout [6]. Hence, using a triangular spectrum (see Fig. 1) in order to simplify the proposed modelling, it comes:

$$\tau_i = 10^{n_i}; \quad n_i = n_c - n_0 + (i - 1)\Delta; \quad \Delta = \frac{2n_0}{n_b - 1} \quad (14)$$

with n_c a user defined relaxation times number and Δ the time interval between two relaxation times, and:

$$\begin{aligned} \mu_i &= +a[n_i - (n_c - n_0)] & \text{if } n_i \in [(n_c - n_0)n_c] \\ \mu_i &= -a[n_i - (n_c + n_0)] & \text{if } n_i \in [n_c(n_c + n_0)] \end{aligned} \quad (15)$$

For the normalisation condition:

$$\sum_{i=1}^{n_b} \mu_i = 1 \quad (16)$$

the slope of the triangle edges is given by:

$$a = \frac{2}{n_0(n_b - 1)} \quad (17)$$

In order to develop a satisfactory viscous modelling at a high stress levels, the so constructed linear viscoelastic model is complemented by a viscoplastic one.

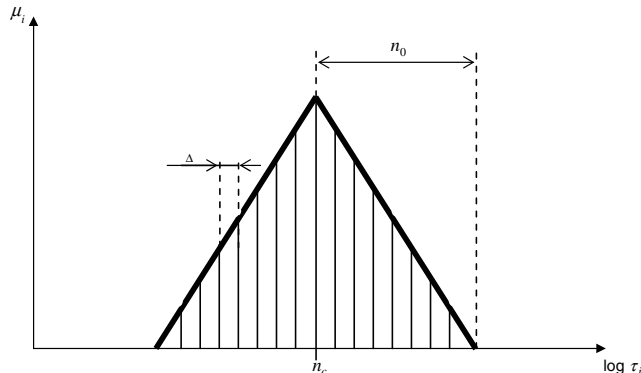


Fig. 1. Triangular spectrum distribution of the relaxation times.

2.2. Viscoplastic behaviour

A generalised Norton-type model integrating the concept of the elastic domain [7] is used to report the plastic strains delay in the equivalent virgin material. This model is based on a kinematics hardening, usually used when the material is submitted to cyclic loading, and on a constant yield stress. For polymer-based materials, a same yield stress is used for both classical plasticity and viscoplasticity. Moreover, the elastic and viscoplastic behaviours are assumed to be independent for the considered loading rates and the restoring phenomena negligible.

In the absence of viscoelastic and plastic flows, the state of the material is assumed to be completely defined by the elastic strains $\underline{\varepsilon}^e$ and a tensorial hardening variable $\underline{\alpha}_3$. The Clausius–Duhem inequality gives in this case the following state law and intrinsic dissipation In_{vp} :

$$\hat{\underline{\sigma}} = \rho \frac{\partial \hat{\psi}}{\partial \underline{\varepsilon}^e}, \quad \text{In}_{\text{vp}} = {}^T \underline{\dot{\varepsilon}}^{\text{vp}} \hat{\underline{\sigma}} - {}^T \underline{\dot{\alpha}}_3 \underline{X}_3 \geq 0 \quad (18)$$

$\underline{X}_3 = \rho \partial \hat{\psi} / \partial \underline{\alpha}_3$ being the thermodynamic force associated with $\underline{\alpha}_3$, $\underline{\dot{\varepsilon}}^{\text{vp}}$ represents the viscoplastic strain rate tensor (the total strains $\underline{\varepsilon}$ are composed of an elastic part $\underline{\varepsilon}^e$ and a viscoplastic part $\underline{\varepsilon}^{\text{vp}}$ i.e. $\underline{\varepsilon} = \underline{\varepsilon}^e + \underline{\varepsilon}^{\text{vp}}$).

$\hat{\psi}$ is chosen of the following form when neither plasticity nor viscoelasticity are considered:

$$\hat{\psi}(\underline{\varepsilon}^e, \underline{\alpha}_3) = \frac{1}{2\rho} {}^T \underline{\varepsilon}^e \underline{A} \underline{\varepsilon}^e + \frac{\delta_3}{2\rho} {}^T \underline{\alpha}_3 \underline{\alpha}_3 \quad (19)$$

what leads to a classical linear kinematics hardening, δ_3 being a material parameter:

$$\underline{X}_3 = \delta_3 \underline{\alpha}_3 \quad (20)$$

Assuming a normal dissipative process [2,3], the kinetics variables $(\underline{\dot{\varepsilon}}^{\text{vp}}, \underline{\dot{\alpha}}_3)$ associated with a given set of thermodynamic forces $(\hat{\underline{\sigma}}, \underline{X}_3)$ belong to the subdifferential of a non-negative continuous convex function $\Gamma(\hat{\underline{\sigma}}, \underline{X}_3)$ i.e. [8]

$${}^T \underline{\dot{\varepsilon}}^{\text{vp}} (\hat{\underline{\sigma}} - \hat{\underline{\sigma}}^*) - {}^T \underline{\dot{\alpha}}_3 (\underline{X}_3 - \underline{X}_3^*) \geq \Gamma(\hat{\underline{\sigma}}, \underline{X}_3) - \Gamma(\hat{\underline{\sigma}}^*, \underline{X}_3^*), \quad \forall [(\hat{\underline{\sigma}}^*, \underline{X}_3^*), (\hat{\underline{\sigma}}, \underline{X}_3)] \quad (21)$$

Hence, introducing the following maximum dissipation principle [1]:

$$\text{In}_{\text{vp}}^r(\hat{\underline{\sigma}}, \underline{X}_3; \underline{\dot{\varepsilon}}^{\text{vp}}, \underline{\dot{\alpha}}_3) = \max_{\forall (\hat{\underline{\sigma}}^*, \underline{X}_3^*)} \text{In}_{\text{vp}}^r(\hat{\underline{\sigma}}^*, \underline{X}_3^*; \underline{\dot{\varepsilon}}^{\text{vp}}, \underline{\dot{\alpha}}_3) \quad (22)$$

with

$$\text{In}_{\text{vp}}^r(\hat{\underline{\sigma}}, \underline{X}_3; \underline{\dot{\varepsilon}}^{\text{vp}}, \underline{\dot{\alpha}}_3) = {}^T \underline{\dot{\varepsilon}}^{\text{vp}} \hat{\underline{\sigma}} - {}^T \underline{\dot{\alpha}}_3 \underline{X}_3 - \Gamma(\hat{\underline{\sigma}}, \underline{X}_3) \quad (23)$$

it comes from the optimality conditions of $-\text{In}_{\text{vp}}^r$:

$$\left. \frac{\partial(-\text{In}_{\text{vp}}^r)}{\partial \hat{\underline{\sigma}}} \right|_{(\hat{\underline{\sigma}}, \underline{X}_3)} = -\underline{\dot{\varepsilon}}^{\text{vp}} + \left. \frac{\partial \Gamma}{\partial \hat{\underline{\sigma}}} \right|_{(\hat{\underline{\sigma}}, \underline{X}_3)} = 0, \quad \left. \frac{\partial(-\text{In}_{\text{vp}}^r)}{\partial \underline{X}_3} \right|_{(\hat{\underline{\sigma}}, \underline{X}_3)} = \underline{\dot{\alpha}}_3 + \left. \frac{\partial \Gamma}{\partial \underline{X}_3} \right|_{(\hat{\underline{\sigma}}, \underline{X}_3)} = 0 \quad (24)$$

The viscoplasticity can hence be interpreted as a regularisation of the classical time-independent plasticity [9,10]: the maximum viscoplastic dissipation is represented by a regularised function $\text{In}_{\text{vp}}^r(\hat{\underline{\sigma}}, \underline{X}_3; \underline{\dot{\varepsilon}}^{\text{vp}}, \underline{\dot{\alpha}}_3)$. The admissible thermodynamic forces field is then enlarged since, contrary to the classical plasticity, the viscoplastic flow take place for stresses outside of the elastic domain $\{\hat{\underline{\sigma}}, \underline{X}_3 / f_{\text{vp}}(\hat{\underline{\sigma}}, \underline{X}_3) \leq 0\}$. So:

$$\Gamma(\hat{\underline{\sigma}}, \underline{X}_3) = \begin{cases} \hat{\Gamma} & \text{if } f_{\text{vp}} > 0 \\ 0 & \text{if } f_{\text{vp}} \leq 0 \end{cases} \quad (25)$$

Choosing Γ such as:

$$\Gamma(\hat{\underline{\sigma}}, \underline{X}_3) = \hat{\Gamma}(f_{\text{vp}}) = K \left[\frac{1}{N+1} (f_{\text{vp}})^{N+1} \right] = K \tilde{\Gamma}(f_{\text{vp}}); \quad \langle f_{\text{vp}} \rangle = \frac{1}{2} (f_{\text{vp}} + |f_{\text{vp}}|) \quad (26)$$

it comes:

$$\underline{\dot{\varepsilon}}^{\text{vp}} = K \langle f_{\text{vp}} \rangle^N \frac{\partial f_{\text{vp}}}{\partial \hat{\underline{\sigma}}}, \quad \underline{\dot{\alpha}}_3 = -K \langle f_{\text{vp}} \rangle^N \frac{\partial f_{\text{vp}}}{\partial \underline{X}_3} \quad (27)$$

N is a parameter characterising the material rate-sensitivity and K an other parameter which can be regarded as a penalty coefficient [11,12], $\tilde{\Gamma}(f_{\text{vp}})$ playing the role of a penalty function for stresses outside the elastic domain. The classical time-independent plasticity model is recovered when $K \rightarrow \infty$. In this case, the functional $\Gamma(f_{\text{vp}})$ converges to the indicator function of the elastic domain.

In the present study, the elastic domain is defined by the following yield function:

$$f_{vp}(\hat{\underline{\boldsymbol{\varepsilon}}}, \underline{\boldsymbol{X}}_3) = \overline{(\hat{\underline{\boldsymbol{\varepsilon}}} - \underline{\boldsymbol{X}}_3)} - \tau_0; \quad \overline{(\hat{\underline{\boldsymbol{\varepsilon}}} - \underline{\boldsymbol{X}}_3)} = \sqrt{\text{T}(\hat{\underline{\boldsymbol{\varepsilon}}} - \underline{\boldsymbol{X}}_3) \underline{\underline{\boldsymbol{M}}} (\hat{\underline{\boldsymbol{\varepsilon}}} - \underline{\boldsymbol{X}}_3)} \quad (28)$$

where τ_0 is a constant yield stress and $\underline{\underline{\boldsymbol{M}}}$ a fourth order tensor describing the anisotropy of plastic [1] and viscoplastic flows associated with friction between the flaw walls.

With respect to the reference frame R_f , the yield stress is reached by shearing in the planes (\vec{x}_1, \vec{x}_2) and (\vec{x}_2, \vec{x}_3) [1]. Hence:

$$\underline{\underline{\boldsymbol{M}}} = \begin{bmatrix} 0 & 0 & 0 & 0 & 0 & 0 \\ 0 & 0 & 0 & 0 & 0 & 0 \\ 0 & 0 & 0 & 0 & 0 & 0 \\ 0 & 0 & 0 & 1 & 0 & 0 \\ 0 & 0 & 0 & 0 & 0 & 0 \\ 0 & 0 & 0 & 0 & 0 & 1 \end{bmatrix} \quad (29)$$

$\underline{\underline{\boldsymbol{M}}}^{-1}$ being positive definite, it induces an inner product $\langle \underline{(\cdot)}, \underline{(\cdot)} \rangle_M = \text{T}(\underline{(\cdot)}) \underline{\underline{\boldsymbol{M}}}^{-1} \underline{(\cdot)}$ and an associated norm $\| \underline{(\cdot)} \|_M = \sqrt{\langle \underline{(\cdot)}, \underline{(\cdot)} \rangle_M}$.

Defining a viscoplastic multiplier $\dot{\lambda}_{vp}$ homogeneous to an equivalent viscoplastic strain rate such as:

$$\dot{\lambda}_{vp} = \| \dot{\underline{\boldsymbol{\varepsilon}}}^{vp} \|_M \quad (30)$$

the following ‘‘dynamic’’ yield function can be introduced by taking account of Eq. (27a):

$$f_{vp}^{dyn}(\hat{\underline{\boldsymbol{\varepsilon}}}, \underline{\boldsymbol{X}}_3; \dot{\lambda}_{vp}) = f_{vp}(\hat{\underline{\boldsymbol{\varepsilon}}}, \underline{\boldsymbol{X}}_3) - \left(\frac{\dot{\lambda}_{vp}}{K} \right)^{1/N} \quad (31)$$

It verifies:

$$\begin{aligned} f_{vp}^{dyn} &\leq 0 && \text{if } f_{vp} \leq 0 \\ f_{vp}^{dyn} &= 0 && \text{if } f_{vp} > 0 \end{aligned} \quad (32)$$

As illustrated by the authors in [13], the concept of ‘‘dynamic’’ yield function allows a unified treatment of plastic and viscoplastic behaviours by suitably generalising the approach exploited in the classical time-independent plasticity (see box 2). Such a function has been used in [14] where a continuous viscoplastic formulation is presented, and an analytical viscoplastic tangent operator is developed in [15] under some restrictive assumptions concerning the second rate of $\dot{\lambda}_{vp}$ resulting from the consistency condition $\dot{f}_{vp}^{dyn} = 0$. In [12], the relation between the viscoplastic multiplier $\dot{\lambda}_{vp}$ and the yield function f_{vp} is established for various viscoplastic models.

3. Instantaneous and creep strains

Assuming that the state of the equivalent virgin material is completely defined by the elastic strains $\underline{\boldsymbol{\varepsilon}}^e$, a set of second order tensors $\underline{\boldsymbol{\xi}}_i$ ($i \in N$) corresponding to viscoelastic flow elementary mechanisms, a scalar hardening variable α and three tensorial hardening variables $\underline{\boldsymbol{\alpha}}_j$ ($j = 1, 2$ and 3), the Clausius–Duhem inequality gives the following state law and intrinsic dissipation In:

$$\begin{aligned} \hat{\underline{\boldsymbol{\sigma}}} &= \rho \frac{\partial}{\partial \underline{\boldsymbol{\varepsilon}}^e} \hat{\psi}(\underline{\boldsymbol{\varepsilon}}^e, \underline{\boldsymbol{\xi}}_i, \alpha, \underline{\boldsymbol{\alpha}}_j), \\ \text{In} &= \text{In}_{ve}(\hat{\underline{\boldsymbol{\sigma}}}, \underline{\boldsymbol{\gamma}}_j; \dot{\underline{\boldsymbol{\varepsilon}}}^{ve}, \dot{\underline{\boldsymbol{\xi}}}_i) + \text{In}_p(\hat{\underline{\boldsymbol{\sigma}}}, \underline{\boldsymbol{X}}_1, \underline{\boldsymbol{X}}_2, R; \dot{\underline{\boldsymbol{\varepsilon}}}^p, \dot{\underline{\boldsymbol{\alpha}}}_1, \dot{\underline{\boldsymbol{\alpha}}}_2, \dot{\alpha}) \\ &\quad + \text{In}_{vp}(\hat{\underline{\boldsymbol{\sigma}}}, \underline{\boldsymbol{X}}_3, \dot{\underline{\boldsymbol{\varepsilon}}}^{vp}, \dot{\underline{\boldsymbol{\alpha}}}_3) \geq 0 \end{aligned} \quad (33)$$

In_p is the intrinsic dissipation plastic component established in [1], where $\underline{\boldsymbol{X}}_1$, $\underline{\boldsymbol{X}}_2$ and R are the thermodynamic forces associated with $\underline{\boldsymbol{\alpha}}_1$, $\underline{\boldsymbol{\alpha}}_2$ and α respectively, and $\dot{\underline{\boldsymbol{\varepsilon}}}^p$ the plastic strain rate tensor (the total strains $\underline{\boldsymbol{\varepsilon}}$ are composed of an elastic part $\underline{\boldsymbol{\varepsilon}}^e$, a viscoelastic part $\underline{\boldsymbol{\varepsilon}}^{ve}$, a plastic part $\underline{\boldsymbol{\varepsilon}}^p$ and a viscoplastic part $\underline{\boldsymbol{\varepsilon}}^{vp}$ i.e. $\underline{\boldsymbol{\varepsilon}} = \underline{\boldsymbol{\varepsilon}}^e + \underline{\boldsymbol{\varepsilon}}^{ve} + \underline{\boldsymbol{\varepsilon}}^p + \underline{\boldsymbol{\varepsilon}}^{vp}$).

Each component In_{ve} (Eq. (2b)), In_p and In_{vp} Eq. (18b) being independent of the kinetics variables whose depend the two others, three uncoupled dissipative processes can be defined:

$$\text{In}_{ve}(\hat{\underline{\boldsymbol{\sigma}}}, \underline{\boldsymbol{\gamma}}_j; \dot{\underline{\boldsymbol{\varepsilon}}}^{ve}, \dot{\underline{\boldsymbol{\xi}}}_i) \geq 0, \quad \text{In}_p(\hat{\underline{\boldsymbol{\sigma}}}, \underline{\boldsymbol{X}}_1, \underline{\boldsymbol{X}}_2, R; \dot{\underline{\boldsymbol{\varepsilon}}}^p, \dot{\underline{\boldsymbol{\alpha}}}_1, \dot{\underline{\boldsymbol{\alpha}}}_2, \dot{\alpha}) \geq 0, \quad \text{In}_{vp}(\hat{\underline{\boldsymbol{\sigma}}}, \underline{\boldsymbol{X}}_3, \dot{\underline{\boldsymbol{\varepsilon}}}^{vp}, \dot{\underline{\boldsymbol{\alpha}}}_3) \geq 0 \quad (34)$$

what allows a simple superposition of the constitutive models built through the previous sections (see [1, Sections 2.1 and 2.2]) in order to take account for instantaneous and creep strains in the material (see box 3).

4. Integration algorithm of the layer behaviour

Within an incremental method associated with the Newton's iterative scheme, the basic problem is to update the state of the material in a fashion consistent with the constitutive model knowing the total incremental strains $\Delta \underline{\underline{\varepsilon}}$. So, for the proposed modelling of the elasto-dissipative mechanisms in a layer (see box 1 of [1] and box 3):

$$\{n\underline{\underline{\sigma}}, nD, n\underline{\underline{\xi}}_j, n\underline{\underline{X}}_1, n\underline{\underline{X}}_2, n\underline{\underline{X}}_3\} + \Delta \underline{\underline{\varepsilon}} \rightarrow \{n+1\underline{\underline{\sigma}}, n+1D, n+1\underline{\underline{\xi}}_j, n+1\underline{\underline{X}}_1, n+1\underline{\underline{X}}_2, n+1\underline{\underline{X}}_3\} \quad (35)$$

$n(\cdot)$ meaning the previous convergent quantities and $n+1(\cdot)$ the current ones. The relationships between these quantities i.e. incremental laws, are derived from the model constitutive equations.

4.1. Elastic-viscoelastic incremental laws

The time-integration of the elastic-viscoelastic constitutive equations (see box 1) over the time interval $[t_n, t_{n+1}]$ leads to:

$$n+1\underline{\underline{\hat{\sigma}}} = n\underline{\underline{\hat{\sigma}}} + \underline{\underline{A}}\Delta \underline{\underline{\varepsilon}} - \underline{\underline{A}}\Delta \underline{\underline{\varepsilon}}^{\text{ve}}; \quad \Delta \underline{\underline{\varepsilon}}^{\text{ve}} = \sum_i \Delta \underline{\underline{\xi}}_i \quad (36)$$

By using the generalised trapezoidal or mid-point scheme [16], the elementary kinetics $\underline{\underline{\xi}}_i$ give:

$$\Delta \underline{\underline{\xi}}_i = n+1\underline{\underline{\xi}}_i - n\underline{\underline{\xi}}_i = \frac{\Delta t}{\tau_i} n+1\underline{\underline{\xi}}_i \left[\mu_i \underline{\underline{S}}_{\text{ve}}(n+1\underline{\underline{\hat{\sigma}}}) - n\underline{\underline{\xi}}_i \right] = \frac{\Delta t}{\tau_i} \left[\mu_i \underline{\underline{S}}_{\text{ve}}(n+1\underline{\underline{\hat{\sigma}}}) - n+1\underline{\underline{\xi}}_i \right]; \quad \Delta t = t_{n+1} - t_n \quad (37)$$

where $n+1\underline{\underline{\xi}}_i = (1 - \varsigma)n\underline{\underline{\xi}}_i + \varsigma n+1\underline{\underline{\xi}}_i$; $0 \leq \varsigma \leq 1$.¹

Hence:

$$n+1\underline{\underline{\xi}}_i = \frac{1 - \varepsilon_A(1 - \varsigma)}{(1 + \varepsilon_A\varsigma)} n\underline{\underline{\xi}}_i + \frac{\varepsilon_A \mu_i}{(1 + \varepsilon_A\varsigma)} \underline{\underline{S}}_{\text{ve}}(n+1\underline{\underline{\hat{\sigma}}}); \quad \varepsilon_A = \frac{\Delta t}{\tau_i} \quad (38)$$

and then:

$$\Delta \underline{\underline{\varepsilon}}^{\text{ve}} = \sum_i \frac{\varepsilon_A \mu_i}{1 + \varepsilon_A\varsigma} \underline{\underline{S}}_{\text{ve}}(n+1\underline{\underline{\hat{\sigma}}}) - \sum_i \frac{\varepsilon_A}{1 + \varepsilon_A\varsigma} n\underline{\underline{\xi}}_i \quad (39)$$

Coming back in Eq. (36), it comes finally:

$$n+1\underline{\underline{\hat{\sigma}}} = \underline{\underline{H}} \left[n\underline{\underline{\hat{\sigma}}} + \underline{\underline{A}}\Delta \underline{\underline{\varepsilon}} - \sum_i \frac{\varepsilon_A \mu_i}{1 + \varepsilon_A\varsigma} \right] (1 - \varsigma) \underline{\underline{A}} \underline{\underline{S}}_{\text{ve}}(n\underline{\underline{\hat{\sigma}}}) + \underline{\underline{A}} \sum_i \frac{\varepsilon_A}{1 + \varepsilon_A\varsigma} n\underline{\underline{\xi}}_i; \quad \underline{\underline{H}}^{-1} = \underline{\underline{I}} + \sum_i \frac{\varepsilon_A \mu_i}{1 + \varepsilon_A\varsigma} \underline{\underline{c}} \underline{\underline{A}} \underline{\underline{S}}_{\text{ve}} \quad (40)$$

4.1.1. Accuracy analysis

An accuracy analysis of this numerical model can be performed by comparing the algorithmic and exact stresses using a standard Taylor series expansion in powers of Δt . The expansion of the algorithmic stresses (Eq. (40)) gives:

$$n+1\underline{\underline{\hat{\sigma}}} = n\underline{\underline{\hat{\sigma}}} + \Delta \frac{d}{d\Delta} (n+1\underline{\underline{\hat{\sigma}}}) \Big|_{\Delta=0} + \frac{1}{2} \Delta^2 \frac{d^2}{d\Delta^2} (n+1\underline{\underline{\hat{\sigma}}}) \Big|_{\Delta=0} + \dots; \quad \Delta \equiv \Delta t \quad (41)$$

where:

$$\begin{aligned} \frac{d}{d\Delta} (n+1\underline{\underline{\hat{\sigma}}}) \Big|_{\Delta=0} &= \underline{\underline{A}} n \dot{\underline{\underline{\varepsilon}}} - \underline{\underline{A}} \sum_i \frac{1}{\tau_i} \left[\mu_i \underline{\underline{S}}_{\text{ve}}(n\underline{\underline{\hat{\sigma}}}) - n\underline{\underline{\xi}}_i \right] \\ \frac{d^2}{d\Delta^2} (n+1\underline{\underline{\hat{\sigma}}}) \Big|_{\Delta=0} &= \underline{\underline{A}} n \ddot{\underline{\underline{\varepsilon}}} - 2\varsigma \underline{\underline{A}} \sum_i \frac{\mu_i}{\tau_i} \underline{\underline{S}}_{\text{ve}} \underline{\underline{A}} \left\{ n \dot{\underline{\underline{\varepsilon}}} - \sum_i \frac{1}{\tau_i} \left[\mu_i \underline{\underline{S}}_{\text{ve}}(n\underline{\underline{\hat{\sigma}}}) - n\underline{\underline{\xi}}_i \right] \right\} + 2\varsigma \underline{\underline{A}} \sum_i \frac{1}{\tau_i^2} \left[\mu_i \underline{\underline{S}}_{\text{ve}}(n\underline{\underline{\hat{\sigma}}}) - n\underline{\underline{\xi}}_i \right] \end{aligned} \quad (42)$$

¹ The generalised trapezoidal and mid-point schemes are equivalent in this case.

Compared to the following expansion of the exact solution:

$${}_{n+1}\hat{\underline{\sigma}} = {}_n\hat{\underline{\sigma}} + \Delta_n \dot{\hat{\underline{\sigma}}} + \frac{1}{2} \Delta_n^2 \ddot{\hat{\underline{\sigma}}} + \dots \quad (43)$$

where:

$$\begin{aligned} \dot{\hat{\underline{\sigma}}} &= \underline{A}_n \dot{\underline{\varepsilon}} - \underline{A} \sum_i \frac{1}{\tau_i} \left[\mu_i \underline{S}_{ve}({}_n\hat{\underline{\sigma}}) - {}_n\dot{\underline{\xi}}_i \right] \\ \ddot{\hat{\underline{\sigma}}} &= \underline{A}_n \ddot{\underline{\varepsilon}} - \underline{A} \sum_i \frac{\mu_i}{\tau_i} \underline{S}_{ve} \underline{A} \left\{ {}_n\dot{\underline{\varepsilon}} - \sum_i \frac{1}{\tau_i} \left[\mu_i \underline{S}_{ve}({}_n\hat{\underline{\sigma}}) - {}_n\dot{\underline{\xi}}_i \right] \right\} + \underline{A} \sum_i \frac{1}{\tau_i^2} \left[\mu_i \underline{S}_{ve}({}_n\hat{\underline{\sigma}}) - {}_n\dot{\underline{\xi}}_i \right] \end{aligned} \quad (44)$$

it shows a second order accuracy for $\varsigma = 1/2$ in the usual sense of the local truncation error.

4.1.2. Stability analysis

It is now well established that the notion of B-stability [17–21] provides a relevant definition of the non-linear stability in the sense that arbitrary perturbations in the initial conditions for an initial value problem are attenuated by the used algorithm. This notion needs the identification of a “natural norm” for the integrated continuum problem relative to which the crucial contractivity property can be verified.

Consider the following standard problem of evolution obtained from the viscoelastic constitutive equations (see box 1) and Eq. (6):

$$\dot{\underline{\Sigma}} = \underline{G}(\dot{\underline{E}} - \dot{\underline{\Xi}}) = f[\underline{\Sigma}(t=0); t]; \quad \underline{\Sigma}(t=0) = \underline{\Sigma}_0 \quad (45)$$

where:

$$\underline{\Sigma} = \begin{pmatrix} \hat{\underline{\sigma}} \\ \underline{\chi}_1 \\ \underline{\chi}_2 \\ \vdots \\ \underline{\chi}_i \\ \vdots \end{pmatrix}, \quad \dot{\underline{E}} = \begin{pmatrix} \dot{\underline{\varepsilon}} \\ \underline{0} \\ \underline{0} \\ \vdots \\ \underline{0} \\ \vdots \end{pmatrix}, \quad \dot{\underline{\Xi}} = \begin{pmatrix} \sum_i \dot{\underline{\xi}}_i \\ -\dot{\underline{\xi}}_1 \\ -\dot{\underline{\xi}}_2 \\ \vdots \\ -\dot{\underline{\xi}}_i \\ \vdots \end{pmatrix}, \quad \underline{G} = \begin{bmatrix} \underline{A} & \underline{0} & \dots & & \underline{0} \\ \underline{0} & \frac{1}{\mu_1} \underline{A}_{ve} & & & \vdots \\ \vdots & & \frac{1}{\mu_2} \underline{A}_{ve} & & \vdots \\ & & & \ddots & \vdots \\ \underline{0} & \dots & & \dots & \frac{1}{\mu_i} \underline{A}_{ve} & \underline{0} \\ & & & & & \ddots \end{bmatrix} \quad (46)$$

\underline{G}^{-1} being positive definite, it induces an inner product $\langle (\cdot), (\cdot) \rangle_G = \text{Tr}(\underline{G}^{-1}(\cdot)(\cdot))$ and an associated norm $\|(\cdot)\|_G = \sqrt{\langle (\cdot), (\cdot) \rangle_G}$. From Eq. (3), it can be easily verified that $\rho \| \underline{\Sigma} \|_G^2 / 2$ corresponds to the dual specific free energy function. The notion of B-stability could then be exploited for the considered viscoelasticity if the evolution equations Eq. (45) are contractive relatively to the norm $\|(\cdot)\|_G$ in the sense that [20]:

$$\frac{d}{dt} \| \underline{\Sigma} - \underline{\Sigma}' \|_G^2 = 2 \text{Tr}(\underline{\Sigma} - \underline{\Sigma}') \underline{G}^{-1}(\dot{\underline{\Sigma}} - \dot{\underline{\Sigma}}') \leq 0 \quad \forall t \quad (47)$$

$\underline{\Sigma}$ and $\underline{\Sigma}'$ being solutions corresponding to two different initial conditions $\underline{\Sigma}_0$ and $\underline{\Sigma}'_0$ respectively, for a given strain rate tensor $\dot{\underline{E}}$.

From Eqs. (45) and (46):

$$\begin{aligned} \frac{d}{dt} \| \underline{\Sigma} - \underline{\Sigma}' \|_G^2 &= 2 \text{Tr} \left(\sum_i \dot{\underline{\xi}}_i - \sum_i \dot{\underline{\xi}}'_i \right) (\hat{\underline{\sigma}} - \hat{\underline{\sigma}}') + 2 \sum_i \text{Tr}(\dot{\underline{\xi}}_i - \dot{\underline{\xi}}'_i) (\underline{\chi}_i - \underline{\chi}'_i) \\ &= 2 \sum_i \text{Tr} \dot{\underline{\xi}}_i \left[(\hat{\underline{\sigma}} - \hat{\underline{\sigma}}') - (\underline{\chi}_i - \underline{\chi}'_i) \right] + 2 \sum_i \text{Tr} \dot{\underline{\xi}}_i \left[(\hat{\underline{\sigma}}' - \hat{\underline{\sigma}}) - (\underline{\chi}'_i - \underline{\chi}_i) \right] \end{aligned} \quad (48)$$

Introducing the dual potential Ω^* of the viscoelastic dissipation potential $\Omega = \Pi_{ve}/2$ (Eq. (11)) such as:

$$\Omega^*(\hat{\underline{\sigma}}, \underline{\chi}_i) = \sup_{\dot{\underline{\xi}}_i} \left\{ \text{Tr} \dot{\underline{\xi}}_i (\hat{\underline{\sigma}} - \underline{\chi}_i) - \frac{1}{2} \frac{\tau_i}{\mu_i} \left(\text{Tr} \dot{\underline{\xi}}_i \underline{A}_{ve} \dot{\underline{\xi}}_i \right) \right\} = \frac{1}{2} \frac{\mu_i}{\tau_i} \left[\text{Tr}(\hat{\underline{\sigma}} - \underline{\chi}_i) \underline{S}_{ve}(\hat{\underline{\sigma}} - \underline{\chi}_i) \right] \quad (49)$$

it comes (Ω^* is a convex function):

$$\Omega^*(\hat{\boldsymbol{\sigma}}^*, \boldsymbol{\chi}_i^*) - \Omega^*(\hat{\boldsymbol{\sigma}}, \boldsymbol{\chi}_i) \geq \mathbf{T} \Delta \underline{\boldsymbol{\xi}}_i \left[(\hat{\boldsymbol{\sigma}}^* - \hat{\boldsymbol{\sigma}}) - (\boldsymbol{\chi}_i^* - \boldsymbol{\chi}_i) \right] \quad \forall [(\hat{\boldsymbol{\sigma}}, \hat{\boldsymbol{\sigma}}^*), (\boldsymbol{\chi}_i, \boldsymbol{\chi}_i^*)] \quad (50)$$

and then:

$$\frac{d}{dt} \|\underline{\boldsymbol{\Sigma}} - \underline{\boldsymbol{\Sigma}}^*\|_G^2 \leq 2 \sum_i \left[\Omega^*(\hat{\boldsymbol{\sigma}}, \boldsymbol{\chi}_i) - \Omega^*(\hat{\boldsymbol{\sigma}}^*, \boldsymbol{\chi}_i^*) \right] + 2 \sum_i \left[\Omega^*(\hat{\boldsymbol{\sigma}}^*, \boldsymbol{\chi}_i^*) - \Omega^*(\hat{\boldsymbol{\sigma}}, \boldsymbol{\chi}_i) \right] = 0 \quad (51)$$

The contractivity property being so established on the assumption of convexity of the dual potential Ω^* , the algorithm leading to Eq. (40) is said B-stable if the following discrete counterpart Eq. (47) is verified:

$$\|_{n+1}\underline{\boldsymbol{\Sigma}} - n_{+1}\underline{\boldsymbol{\Sigma}}^*\|_G^2 \leq \|_n\underline{\boldsymbol{\Sigma}} - n\underline{\boldsymbol{\Sigma}}^*\|_G^2 \quad (52)$$

$_{n+1}\underline{\boldsymbol{\Sigma}}$ and $_{n+1}\underline{\boldsymbol{\Sigma}}^*$ are two algorithmic solutions corresponding to the initial conditions $_n\underline{\boldsymbol{\Sigma}}$ and $_n\underline{\boldsymbol{\Sigma}}^*$ respectively, for a given strain increment $\Delta \underline{\boldsymbol{E}}$. Obtained from the numerical integration of Eq. (45)² such as:

$$_{n+1}\underline{\boldsymbol{\Sigma}} = _n\underline{\boldsymbol{\Sigma}} + \underline{\underline{\mathbf{G}}}(\Delta \underline{\boldsymbol{E}} - \Delta \underline{\boldsymbol{E}}^*), \quad _{n+1}\underline{\boldsymbol{\Sigma}}^* = _n\underline{\boldsymbol{\Sigma}}^* + \underline{\underline{\mathbf{G}}}(\Delta \underline{\boldsymbol{E}} - \Delta \underline{\boldsymbol{E}}^*) \quad (53)$$

where:

$$\Delta \underline{\boldsymbol{E}} = \begin{pmatrix} \sum_i \Delta \underline{\boldsymbol{\xi}}_i \\ -\Delta \underline{\boldsymbol{\xi}}_1 \\ -\Delta \underline{\boldsymbol{\xi}}_2 \\ \vdots \\ -\Delta \underline{\boldsymbol{\xi}}_i \\ \vdots \end{pmatrix} = \begin{pmatrix} \sum_i \Delta t \frac{\mu_i}{\tau_i} \underline{\underline{\mathbf{S}}}_{\text{ve}}(_{n+\varsigma}\hat{\boldsymbol{\sigma}} - _{n+\varsigma}\boldsymbol{\chi}_i) \\ -\Delta t \frac{\mu_1}{\tau_1} \underline{\underline{\mathbf{S}}}_{\text{ve}}(_{n+\varsigma}\hat{\boldsymbol{\sigma}} - _{n+\varsigma}\boldsymbol{\chi}_1) \\ -\Delta t \frac{\mu_2}{\tau_2} \underline{\underline{\mathbf{S}}}_{\text{ve}}(_{n+\varsigma}\hat{\boldsymbol{\sigma}} - _{n+\varsigma}\boldsymbol{\chi}_2) \\ \vdots \\ -\Delta t \frac{\mu_i}{\tau_i} \underline{\underline{\mathbf{S}}}_{\text{ve}}(_{n+\varsigma}\hat{\boldsymbol{\sigma}} - _{n+\varsigma}\boldsymbol{\chi}_i) \\ \vdots \end{pmatrix}; \quad \Delta t = t_{n+1} - t_n, \quad 0 \leq \varsigma \leq 1 \quad (54)$$

Eq. (52) is equivalent to:

$$\|_{n+1}\underline{\boldsymbol{\Sigma}} - n_{+1}\underline{\boldsymbol{\Sigma}}^*\|_G^2 - \|_n\underline{\boldsymbol{\Sigma}} - n\underline{\boldsymbol{\Sigma}}^*\|_G^2 = 2^T \mathbf{T} \mathbf{T} (\Delta \underline{\boldsymbol{E}}^* - \Delta \underline{\boldsymbol{E}}) + 2^T \mathbf{T} \mathbf{T} (\Delta \underline{\boldsymbol{E}} - \Delta \underline{\boldsymbol{E}}^*) + \left\| \underline{\underline{\mathbf{G}}}(\Delta \underline{\boldsymbol{E}}^* - \Delta \underline{\boldsymbol{E}}) \right\|_G^2 \leq 0 \quad (55)$$

with:

$$\left\| \underline{\underline{\mathbf{G}}}(\Delta \underline{\boldsymbol{E}}^* - \Delta \underline{\boldsymbol{E}}) \right\|_G^2 = \mathbf{T} [(_{n+1}\underline{\boldsymbol{\Sigma}} - _n\underline{\boldsymbol{\Sigma}}) - (_{n+1}\underline{\boldsymbol{\Sigma}}^* - _n\underline{\boldsymbol{\Sigma}}^*)] (\Delta \underline{\boldsymbol{E}}^* - \Delta \underline{\boldsymbol{E}}) \quad (56)$$

Hence:

$$\begin{aligned} \|_{n+1}\underline{\boldsymbol{\Sigma}} - n_{+1}\underline{\boldsymbol{\Sigma}}^*\|_G^2 - \|_n\underline{\boldsymbol{\Sigma}} - n\underline{\boldsymbol{\Sigma}}^*\|_G^2 &= 2^T \mathbf{T} \mathbf{T} (\Delta \underline{\boldsymbol{E}}^* - \Delta \underline{\boldsymbol{E}}) + 2^T \mathbf{T} \mathbf{T} (\Delta \underline{\boldsymbol{E}} - \Delta \underline{\boldsymbol{E}}^*) + (1 - 2\varsigma) \left\| \underline{\underline{\mathbf{G}}}(\Delta \underline{\boldsymbol{E}}^* - \Delta \underline{\boldsymbol{E}}) \right\|_G^2 \\ &= 2 \sum_i \mathbf{T} \Delta \underline{\boldsymbol{\xi}}_i^* [(_{n+\varsigma}\hat{\boldsymbol{\sigma}} - _{n+\varsigma}\hat{\boldsymbol{\sigma}}^*) - (_{n+\varsigma}\boldsymbol{\chi}_i - _{n+\varsigma}\boldsymbol{\chi}_i^*)] + 2 \sum_i \mathbf{T} \Delta \underline{\boldsymbol{\xi}}_i [(_{n+\varsigma}\hat{\boldsymbol{\sigma}} - _{n+\varsigma}\hat{\boldsymbol{\sigma}}) \\ &\quad - (_{n+\varsigma}\boldsymbol{\chi}_i^* - _{n+\varsigma}\boldsymbol{\chi}_i)] + (1 - 2\varsigma) \left\| \underline{\underline{\mathbf{G}}}(\Delta \underline{\boldsymbol{E}}^* - \Delta \underline{\boldsymbol{E}}) \right\|_G^2 \end{aligned} \quad (57)$$

The time-integration of the convexity condition (Eq. (50)) following the generalised trapezoidal and mid-point rules over $[t_n, t_{n+1}]$ giving respectively:

$$\begin{aligned} \Delta t \left[\mathbf{T} \Delta \underline{\boldsymbol{\xi}}_i^* \left[(_{n+\varsigma}\hat{\boldsymbol{\sigma}} - _{n+\varsigma}\hat{\boldsymbol{\sigma}}^*) - (_{n+\varsigma}\boldsymbol{\chi}_i - _{n+\varsigma}\boldsymbol{\chi}_i^*) \right] \right] &\geq \mathbf{T} \Delta \underline{\boldsymbol{\xi}}_i^* \left[(_{n+\varsigma}\hat{\boldsymbol{\sigma}} - _{n+\varsigma}\hat{\boldsymbol{\sigma}}^*) - (_{n+\varsigma}\boldsymbol{\chi}_i - _{n+\varsigma}\boldsymbol{\chi}_i^*) \right] \\ \Delta t \left[\mathbf{T} \Delta \underline{\boldsymbol{\xi}}_i \left[(_{n+\varsigma}\hat{\boldsymbol{\sigma}} - _{n+\varsigma}\hat{\boldsymbol{\sigma}}) - (_{n+\varsigma}\boldsymbol{\chi}_i^* - _{n+\varsigma}\boldsymbol{\chi}_i) \right] \right] &\geq \mathbf{T} \Delta \underline{\boldsymbol{\xi}}_i \left[(_{n+\varsigma}\hat{\boldsymbol{\sigma}} - _{n+\varsigma}\hat{\boldsymbol{\sigma}}) - (_{n+\varsigma}\boldsymbol{\chi}_i^* - _{n+\varsigma}\boldsymbol{\chi}_i) \right] \end{aligned} \quad (58)$$

it comes finally:

$$\|_{n+1}\underline{\boldsymbol{\Sigma}} - n_{+1}\underline{\boldsymbol{\Sigma}}^*\|_G^2 - \|_n\underline{\boldsymbol{\Sigma}} - n\underline{\boldsymbol{\Sigma}}^*\|_G^2 \leq (1 - 2\varsigma) \left\| \underline{\underline{\mathbf{G}}}(\Delta \underline{\boldsymbol{E}}^* - \Delta \underline{\boldsymbol{E}}) \right\|_G^2 \quad (59)$$

what allows us to conclude that these two integration schemes applied to the considered viscoelastic constitutive equations are unconditional B-stable for $\varsigma \geq 1/2$.

² This procedure is strictly equivalent to the one used to establish Eq. (40).

4.1.3. Exact integration for creep behaviours

In the particular case of creep behaviours, an exact time-dependent function $\underline{\xi}_i(t)$ can be obtained by solving the following constant coefficients first order differential equation (see box 1):

$$\dot{\underline{\xi}}_i + \frac{1}{\tau_i} \underline{\xi}_i = \frac{\mu_i}{\tau_i} \underline{\mathcal{S}}_{\text{ve}} \hat{\underline{\sigma}} \quad (60)$$

So:

$$\underline{\xi}_i(t) = \mu_i \underline{\mathcal{S}}_{\text{ve}} \hat{\underline{\sigma}} + e^{(-t/\tau_i)} \left[\underline{\xi}_i(t_0) - \mu_i \underline{\mathcal{S}}_{\text{ve}} \hat{\underline{\sigma}} \right] \quad (61)$$

and over the time interval $[t_n, t_{n+1}]$:

$${}_{n+1}\underline{\xi}_i = \mu_i \underline{\mathcal{S}}_{\text{ve}} ({}_n\hat{\underline{\sigma}}) + e^{(-\varepsilon_A)} \left[\underline{\xi}_i - \mu_i \underline{\mathcal{S}}_{\text{ve}} ({}_n\hat{\underline{\sigma}}) \right]; \quad \varepsilon_A = \frac{\Delta t}{\tau_i}; \quad \Delta t = t_{n+1} - t_n \quad (62)$$

From Eqs. (36) and (13), it comes in this case:

$${}_{n+1}\hat{\underline{\sigma}} = {}_n\hat{\underline{\sigma}} + \underline{\underline{A}} \Delta \underline{\underline{\varepsilon}} - \underline{\underline{A}} \sum_i \left[1 + e^{(-\varepsilon_A)} \right] \left[\mu_i \underline{\mathcal{S}}_{\text{ve}} ({}_n\hat{\underline{\sigma}}) - {}_n\underline{\xi}_i \right] \quad (63)$$

4.2. Elasto-viscoplastic incremental laws

The time-integration of the elasto-viscoplastic constitutive equations (see box 2) over the time interval $[t_n, t_{n+1}]$ leads to:

$${}_{n+1}\hat{\underline{\sigma}} = {}_n\hat{\underline{\sigma}} + \underline{\underline{A}} \Delta \underline{\underline{\varepsilon}} - \underline{\underline{A}} \Delta \underline{\underline{\varepsilon}}^{\text{vp}}, \quad {}_{n+1}\underline{\underline{X}}_3 = {}_n\underline{\underline{X}}_3 + \delta_3 \Delta \underline{\underline{\alpha}}_3; \quad \Delta \underline{\underline{\alpha}}_3 = \Delta \underline{\underline{\varepsilon}}^{\text{vp}} \quad (64)$$

By using the generalised trapezoidal and mid-point schemes [16], the viscoplastic strain rate tensor $\dot{\underline{\varepsilon}}^{\text{vp}}$ gives respectively:

$$\begin{aligned} \Delta \underline{\underline{\varepsilon}}^{\text{vp}} &= \Delta t \left[(1 - \varsigma) {}_n\dot{\lambda}_{\text{vp}} \frac{\underline{\underline{M}}({}_n\hat{\underline{\sigma}} - {}_n\underline{\underline{X}}_3)}{({}_n\hat{\underline{\sigma}} - {}_n\underline{\underline{X}}_3)} + \varsigma {}_{n+1}\dot{\lambda}_{\text{vp}} \frac{\underline{\underline{M}}({}_{n+1}\hat{\underline{\sigma}} - {}_{n+1}\underline{\underline{X}}_3)}{({}_{n+1}\hat{\underline{\sigma}} - {}_{n+1}\underline{\underline{X}}_3)} \right]; \\ {}_n\dot{\lambda}_{\text{vp}} &= K \left\langle \overline{({}_n\hat{\underline{\sigma}} - {}_n\underline{\underline{X}}_3)} - \tau_0 \right\rangle^N; \\ {}_{n+1}\dot{\lambda}_{\text{vp}} &= K \left\langle \overline{({}_{n+1}\hat{\underline{\sigma}} - {}_{n+1}\underline{\underline{X}}_3)} - \tau_0 \right\rangle^N \end{aligned} \quad (65)$$

and:

$$\begin{aligned} \Delta \underline{\underline{\varepsilon}}^{\text{vp}} &= \Delta t {}_{n+\varsigma}\dot{\lambda}_{\text{vp}} \frac{\underline{\underline{M}}({}_{n+\varsigma}\hat{\underline{\sigma}} - {}_{n+\varsigma}\underline{\underline{X}}_3)}{({}_{n+\varsigma}\hat{\underline{\sigma}} - {}_{n+\varsigma}\underline{\underline{X}}_3)}; \\ {}_{n+\varsigma}\dot{\lambda}_{\text{vp}} &= K \left\langle \overline{({}_{n+\varsigma}\hat{\underline{\sigma}} - {}_{n+\varsigma}\underline{\underline{X}}_3)} - \tau_0 \right\rangle^N; \\ {}_{n+\varsigma}(\cdot) &= (1 - \varsigma) {}_n(\cdot) + \varsigma {}_{n+1}(\cdot) \end{aligned} \quad (66)$$

with $\Delta t = t_{n+1} - t_n$ and $0 \leq \varsigma \leq 1$. These two algorithms are equivalent for $\varsigma = 0$ and $\varsigma = 1$, otherwise, they lead to different procedures. In particular, the yield condition is assumed to be verified at an intermediate time $t_{n+\varsigma}$ for the generalised mid-point rule i.e. $f_{\text{vp}}({}_{n+\varsigma}\hat{\underline{\sigma}}, {}_{n+\varsigma}\underline{\underline{X}}_3) > 0$ but not necessarily at the end of the time interval.

As shown through Eqs. (65) and (66), the updated variables at the end of the time interval (Eq. (64)) depend on the formal expression of $({}_{n+1}\hat{\underline{\sigma}} - {}_{n+1}\underline{\underline{X}}_3)$. Hence, using:

$$\overline{({}_{n+\varsigma}\hat{\underline{\sigma}} - {}_{n+\varsigma}\underline{\underline{X}}_3)} = \left(\frac{{}_{n+\varsigma}\dot{\lambda}_{\text{vp}}}{K} \right)^{1/N} + \tau_0 \quad (67)$$

at different times, one obtains:

$$\begin{aligned} ({}_{n+1}\hat{\underline{\sigma}} - {}_{n+1}\underline{\underline{X}}_3) &= {}^{\text{tr}}\underline{\underline{T}} \left[{}_n\hat{\underline{\sigma}} + \underline{\underline{A}} \Delta \underline{\underline{\varepsilon}} - {}_n\underline{\underline{X}}_3 - \Delta t \frac{{}_n\dot{\lambda}_{\text{vp}}}{({}_n\dot{\lambda}_{\text{vp}}/K)^{1/N} + \tau_0} (1 - \varsigma) (\underline{\underline{A}} + \delta_3 \underline{\underline{I}}) \underline{\underline{M}}({}_n\hat{\underline{\sigma}} - {}_n\underline{\underline{X}}_3) \right]; \\ {}^{\text{tr}}\underline{\underline{T}}^{-1} &= \underline{\underline{I}} + \Delta t \frac{{}_{n+1}\dot{\lambda}_{\text{vp}}}{({}_{n+1}\dot{\lambda}_{\text{vp}}/K)^{1/N} + \tau_0} \varsigma (\underline{\underline{A}} + \delta_3 \underline{\underline{I}}) \underline{\underline{M}} \end{aligned} \quad (68)$$

for the trapezoidal rule, and for the mid-point one:

$$\begin{aligned}({}_{n+1}\hat{\underline{\boldsymbol{\sigma}}} - {}_{n+1}\underline{\boldsymbol{X}}_3) &= {}^{mi}\underline{\underline{T}} \left[{}_n\hat{\underline{\boldsymbol{\sigma}}} + \underline{\underline{A}} \Delta \underline{\underline{\boldsymbol{\varepsilon}}} - {}_n\underline{\underline{\boldsymbol{X}}}_3 - \Delta t \frac{{}_{n+\zeta}\dot{\lambda}^{vp}}{({}_{n+\zeta}\dot{\lambda}_{vp}/K)^{1/N} + \tau_0} (1 - \zeta) (\underline{\underline{A}} + \delta_3 \underline{\underline{I}}) \underline{\underline{M}} ({}_n\hat{\underline{\boldsymbol{\sigma}}} - {}_n\underline{\underline{\boldsymbol{X}}}_3) \right]; \\ {}^{mi}\underline{\underline{T}}^{-1} &= \underline{\underline{I}} + \Delta t \frac{{}_{n+\zeta}\dot{\lambda}^{vp}}{({}_{n+\zeta}\dot{\lambda}_{vp}/K)^{1/N} + \tau_0} \zeta (\underline{\underline{A}} + \delta_3 \underline{\underline{I}}) \underline{\underline{M}}\end{aligned}\quad (69)$$

Accuracy and non-linear stability analysis of these rules are presented Appendix A. A second order accuracy is established for $\zeta = 1/2$ in the usual sense of the local truncation error and an unconditional B-stability for $\zeta \geq 1/2$ is recovered for the mid-point rule. For the trapezoidal one, the B-stability analysis is not performed herein and remains, to our knowledge, an open problem.

4.3. Generalised elasto-dissipative incremental laws

The time-integration of the elastic–viscoelastic–plastic–viscoplastic constitutive equations (see box 3) over the time interval $[t_n, t_{n+1}]$ leads to:³

$$\begin{aligned}{}_{n+1}\hat{\underline{\boldsymbol{\sigma}}} &= {}_n\hat{\underline{\boldsymbol{\sigma}}} + \underline{\underline{A}} \Delta \underline{\underline{\boldsymbol{\varepsilon}}} - \underline{\underline{A}} \Delta \underline{\underline{\boldsymbol{\varepsilon}}}^{ve} - \underline{\underline{A}} \Delta \underline{\underline{\boldsymbol{\varepsilon}}}^p - \underline{\underline{A}} \Delta \underline{\underline{\boldsymbol{\varepsilon}}}^{vp} \\ {}_{n+1}\underline{\underline{\boldsymbol{X}}}_1 &= {}_n\underline{\underline{\boldsymbol{X}}}_1 + \delta_1 \Delta \underline{\underline{\boldsymbol{\varepsilon}}}^p - \gamma_1 \int_{t_n}^{t_{n+1}} \dot{\lambda}_p \underline{\underline{M}} \underline{\underline{\boldsymbol{X}}}_1 dt \\ {}_{n+1}\underline{\underline{\boldsymbol{X}}}_2 &= {}_n\underline{\underline{\boldsymbol{X}}}_2 + \delta_2 \Delta \underline{\underline{\boldsymbol{\varepsilon}}}^p \\ {}_{n+1}\underline{\underline{\boldsymbol{X}}}_3 &= {}_n\underline{\underline{\boldsymbol{X}}}_3 + \delta_3 \Delta \underline{\underline{\boldsymbol{\varepsilon}}}^{vp}\end{aligned}\quad (70)$$

Without loss of generality, the use of a fully implicit integration, for the sake of simplicity, gives:

$$\begin{aligned}\Delta \underline{\underline{\boldsymbol{\varepsilon}}}^{ve} &= \sum_i \frac{\varepsilon_A \mu_i}{1 + \varepsilon_A} \underline{\underline{S}}_{ve} ({}_{n+1}\hat{\underline{\boldsymbol{\sigma}}}) - \sum_i \frac{\varepsilon_A}{1 + \varepsilon_A} n \underline{\underline{\boldsymbol{\varepsilon}}}_i \\ \Delta \underline{\underline{\boldsymbol{\varepsilon}}}^p &= \frac{\Delta \lambda_p}{\tau_0} \underline{\underline{M}} ({}_{n+1}\hat{\underline{\boldsymbol{\sigma}}} - {}_{n+1}\underline{\underline{\boldsymbol{X}}}) = \frac{\Delta \lambda_p}{\tau_0} \underline{\underline{M}}_{n+1} (\hat{\underline{\boldsymbol{\sigma}}} - \underline{\underline{\boldsymbol{X}}}) \\ \Delta \underline{\underline{\boldsymbol{\varepsilon}}}^{vp} &= \Delta t \frac{{}_{n+1}\dot{\lambda}_{vp}}{({}_{n+1}\dot{\lambda}_{vp}/K)^{1/N} + \tau_0} \underline{\underline{M}} ({}_{n+1}\hat{\underline{\boldsymbol{\sigma}}} - {}_{n+1}\underline{\underline{\boldsymbol{X}}}_3) = \Delta t \frac{{}_{n+1}\dot{\lambda}_{vp}}{({}_{n+1}\dot{\lambda}_{vp}/K)^{1/N} + \tau_0} \underline{\underline{M}}_{n+1} (\hat{\underline{\boldsymbol{\sigma}}} - \underline{\underline{\boldsymbol{X}}}_3)\end{aligned}\quad (71)$$

with Eq. (38):

$$n \underline{\underline{\boldsymbol{\varepsilon}}}_i = \frac{1}{1 + \varepsilon_A} \left[n-1 \underline{\underline{\boldsymbol{\varepsilon}}}_i + \varepsilon_A \mu_i \underline{\underline{S}}_{ve} ({}_n\hat{\underline{\boldsymbol{\sigma}}}) \right]; \quad \varepsilon_A = \frac{\Delta t}{\tau_i}\quad (72)$$

From Eqs. (70b), (70c) and (71b), it comes:

$${}_{n+1}\underline{\underline{\boldsymbol{X}}} = \underline{\underline{A}}_n \underline{\underline{\boldsymbol{X}}}_1 + {}_n\underline{\underline{\boldsymbol{X}}}_2 + \frac{\Delta \lambda_p}{\tau_0} (\delta_1 \underline{\underline{A}} + \delta_2 \underline{\underline{I}}) \underline{\underline{M}}_{n+1} (\hat{\underline{\boldsymbol{\sigma}}} - \underline{\underline{\boldsymbol{X}}}); \quad \underline{\underline{A}}^{-1} = \underline{\underline{I}} + \Delta \lambda_p \gamma_1 \underline{\underline{M}}\quad (73)$$

Hence:

$${}_{n+1}\underline{\underline{\boldsymbol{X}}} = \underline{\underline{Y}} (\underline{\underline{A}}_n \underline{\underline{\boldsymbol{X}}}_1 + {}_n\underline{\underline{\boldsymbol{X}}}_2) + \frac{\Delta \lambda_p}{\tau_0} \underline{\underline{Y}} (\delta_1 \underline{\underline{A}} + \delta_2 \underline{\underline{I}}) \underline{\underline{M}}_{n+1} \hat{\underline{\boldsymbol{\sigma}}}; \quad \underline{\underline{Y}}^{-1} = \underline{\underline{I}} + \frac{\Delta \lambda_p}{\tau_0} (\delta_1 \underline{\underline{A}} + \delta_2 \underline{\underline{I}}) \underline{\underline{M}}\quad (74)$$

and then:

$${}_{n+1}(\hat{\underline{\boldsymbol{\sigma}}} - \underline{\underline{\boldsymbol{X}}}) = \underline{\underline{U}}_{n+1} \hat{\underline{\boldsymbol{\sigma}}} - \underline{\underline{Y}} (\underline{\underline{A}}_n \underline{\underline{\boldsymbol{X}}}_1 + {}_n\underline{\underline{\boldsymbol{X}}}_2); \quad \underline{\underline{U}} = \underline{\underline{I}} - \frac{\Delta \lambda_p}{\tau_0} \underline{\underline{Y}} (\delta_1 \underline{\underline{A}} + \delta_2 \underline{\underline{I}}) \underline{\underline{M}}\quad (75)$$

From Eqs. (70d) and (71c), it comes:

$${}_{n+1}\underline{\underline{\boldsymbol{X}}}_3 = \underline{\underline{Z}}_n \underline{\underline{\boldsymbol{X}}}_3 + \delta_3 \Delta t \frac{{}_{n+1}\dot{\lambda}_{vp}}{({}_{n+1}\dot{\lambda}_{vp}/K)^{1/N} + \tau_0} \underline{\underline{Z}} \underline{\underline{M}}_{n+1} \hat{\underline{\boldsymbol{\sigma}}}; \quad \underline{\underline{Z}}^{-1} = \underline{\underline{I}} + \delta_3 \Delta t \frac{{}_{n+1}\dot{\lambda}_{vp}}{({}_{n+1}\dot{\lambda}_{vp}/K)^{1/N} + \tau_0} \underline{\underline{M}}\quad (76)$$

³ Refer to [1] for more details concerning the plastic modelling (material parameters, plastic multiplier, ...).

and then:

$${}_{n+1}\hat{\underline{\sigma}} - \underline{X}_3 = \underline{V}_{n+1}\hat{\underline{\sigma}} - \underline{Z}_n\underline{X}_3; \quad \underline{V} = \underline{I} - \delta_3 \Delta t \frac{{}_{n+1}\dot{\lambda}_{vp}}{({}_{n+1}\dot{\lambda}_{vp}/K)^{1/N} + \tau_0} \underline{ZM} \quad (77)$$

Coming back in Eq. (70a), one obtains finally:

$$\begin{aligned} {}_{n+1}\hat{\underline{\sigma}} &= \underline{W} \left[{}_n\hat{\underline{\sigma}} + \underline{A}\Delta\varepsilon + \underline{A} \sum_i \frac{\varepsilon_A}{1 + \varepsilon_A} {}_n\underline{\xi}_i + \frac{\Delta\lambda_p}{\tau_0} \underline{AMY}(\underline{A}_n\underline{X}_1 + {}_n\underline{X}_2) + \Delta t \frac{{}_{n+1}\dot{\lambda}_{vp}}{({}_{n+1}\dot{\lambda}_{vp}/K)^{1/N} + \tau_0} \underline{AMZ}_n\underline{X}_3 \right]; \\ \underline{W}^{-1} &= \underline{I} + \sum_i \frac{\varepsilon_A \mu_i}{1 + \varepsilon_A} \underline{AS}_{ve} + \frac{\Delta\lambda_p}{\tau_0} \underline{AMU} + \Delta t \frac{{}_{n+1}\dot{\lambda}_{vp}}{({}_{n+1}\dot{\lambda}_{vp}/K)^{1/N} + \tau_0} \underline{AMV} \end{aligned} \quad (78)$$

Accuracy and stability properties are preserved by a behaviours superposition. Refer to [20] for accuracy and B-stability analysis of classical plasticity.

For a creep behaviour (see Section 4.1.3), this relation becomes:

$$\begin{aligned} {}_{n+1}\hat{\underline{\sigma}} &= \underline{W} \left\{ {}_n\hat{\underline{\sigma}} + \underline{A}\Delta\varepsilon - \underline{A} \sum_i [1 + e^{(-\varepsilon_A)}] [\mu_i \underline{S}_{ve}({}_n\hat{\underline{\sigma}}) - {}_n\underline{\xi}_i] + \frac{\Delta\lambda_p}{\tau_0} \underline{AMY}(\underline{A}_n\underline{X}_1 + {}_n\underline{X}_2) \right. \\ &\quad \left. + \Delta t \frac{{}_{n+1}\dot{\lambda}_{vp}}{({}_{n+1}\dot{\lambda}_{vp}/K)^{1/N} + \tau_0} \underline{AMZ}_n\underline{X}_3 \right\}; \\ \underline{W}^{-1} &= \underline{I} + \frac{\Delta\lambda_p}{\tau_0} \underline{AMU} + \Delta t \frac{{}_{n+1}\dot{\lambda}_{vp}}{({}_{n+1}\dot{\lambda}_{vp}/K)^{1/N} + \tau_0} \underline{AMV} \end{aligned} \quad (79)$$

The Cauchy true stresses are deduced from the effective stresses (Eq. (78) or Eq. (79)) as follows (Eq. (1)):

$${}_{n+1}\underline{\sigma} = \underline{L}_{n+1}\hat{\underline{\sigma}}; \quad \underline{L}^{-1} = \underline{I} + \underline{AH}({}_{n+1}D); \quad {}_{n+1}D = {}_nD + \Delta\lambda_d \quad (80)$$

$\Delta\lambda_d$ being the increment of the damage variable over the time interval $[t_n, t_{n+1}]$.

All these relations can be naturally interpreted as a strain-based multi-step predictor–corrector scheme [22–25]:

- (i) Elastic–viscoelastic prediction in the effective stress space
- (ii) Plastic–viscoplastic correction in the effective stress space
- (iii) Elastic–viscoelastic–plastic–viscoplastic prediction in the true stress space
- (iv) Damage correction in the true stress space

4.4. Multi-step predictor–corrector scheme

4.4.1. Elastic–viscoelastic prediction

An elastic–viscoelastic prediction ${}_{n+1}\hat{\underline{\sigma}}^{\text{trial}}$ for a time step $\Delta t = t_{n+1} - t_n$ is given by Eq. (40) or Eq. (63). It is obtained by freezing plastic and viscoplastic flows i.e. ${}_{n+1}\underline{X}_i = {}_n\underline{X}_i$; $i = 1, 2$ and 3.

In a Kirchhoff shell context as introduced in [1], the zero normal stress assumption is not necessarily verified in the effective stress space i.e. $\hat{\underline{\sigma}}_{33} \neq 0$. Hence:

$$\underline{S}_{ve} = \begin{bmatrix} 0 & 0 & 0 & 0 \\ 0 & \frac{\beta_2}{E_2} & -\beta_{23} \frac{v_{23}}{E_2} & 0 \\ 0 & -\beta_{23} \frac{v_{23}}{E_2} & \frac{\beta_2}{E_2} & 0 \\ 0 & 0 & 0 & \frac{\beta_{12}}{G_{12}} \end{bmatrix} \quad (81)$$

and:

$$\underline{A} = \begin{bmatrix} \frac{1}{E_1} & -\frac{v_{12}}{E_1} & -\frac{v_{12}}{E_1} & 0 \\ -\frac{v_{12}}{E_1} & \frac{1}{E_2} & -\frac{v_{23}}{E_2} & 0 \\ -\frac{v_{12}}{E_1} & -\frac{v_{23}}{E_2} & \frac{1}{E_2} & 0 \\ 0 & 0 & 0 & \frac{1}{G_{12}} \end{bmatrix}^{-1} = \begin{bmatrix} A_{11} & A_{12} & A_{13} & 0 \\ A_{12} & A_{22} & A_{23} & 0 \\ A_{13} & A_{23} & A_{33} & 0 \\ 0 & 0 & 0 & A_{44} \end{bmatrix} \quad (82)$$

The normal strain increment $\Delta\varepsilon_{33}$ is computed from the true stress-strain relationships of the damaged elastic material by freezing its degradation i.e. ${}_{n+1}D = {}_nD$ [1]:

$$\Delta \varepsilon_{33} = \frac{-v_{12}(E_1 + v_{23}E_1(1 - nD))}{E_1 - v_{12}^2 E_2(1 - nD)} \Delta \varepsilon_{11} - \frac{(v_{23}E_1 + v_{12}^2 E_2)(1 - nD)}{E_1 - v_{12}^2 E_2(1 - nD)} \Delta \varepsilon_{22} \quad (83)$$

If the plastic and viscoplastic yield conditions are not violated i.e.

$$f_p(n+\zeta \hat{\underline{\sigma}}^{\text{trial}}, n\underline{X}_1, n\underline{X}_2) < 0, \quad f_{vp}(n+1 \hat{\underline{\sigma}}^{\text{trial}}, n\underline{X}_3) < 0 \quad \text{or} \quad f_{vp}(n+\zeta \hat{\underline{\sigma}}^{\text{trial}}, n\underline{X}_3) < 0; \\ n+\zeta \hat{\underline{\sigma}}^{\text{trial}} = (1 - \zeta)n\hat{\underline{\sigma}} + \zeta n+1 \hat{\underline{\sigma}}^{\text{trial}}, \quad 0 \leq \zeta \leq 1 \quad (84)$$

the current step is considered to be elastic and the trial stresses $n+1 \hat{\underline{\sigma}}^{\text{trial}}$ are admissible and are accepted as the current effective stresses for the given strain increment $\Delta \underline{\varepsilon}$ (where $\Delta \varepsilon_{33}$ is given by Eq. (83)).

4.4.2. Plastic correction

If a plastic correction is necessary, it is performed by using Eq. (78) or Eq. (79) for a fully implicit integration:

$$n+1 \hat{\underline{\sigma}} = \underline{\underline{W}} \left[\underline{\Psi} + \frac{\Delta \lambda_p}{\tau_0} \underline{\underline{AMY}} (\underline{\underline{A}}n\underline{X}_1 + n\underline{X}_2) \right]; \\ \underline{\Psi} = n\hat{\underline{\sigma}} + \underline{\underline{A}}\Delta \underline{\varepsilon} + \underline{\underline{A}} \sum_i \frac{\varepsilon_{\Delta}}{1 + \varepsilon_{\Delta}} n \underline{\underline{\zeta}}_i \neq n+1 \hat{\underline{\sigma}}^{\text{trial}} \quad \text{or} \quad \underline{\Psi} = n+1 \hat{\underline{\sigma}}^{\text{trial}} \quad (85) \\ \underline{\underline{W}}^{-1} = \underline{\underline{I}} + \sum_i \frac{\varepsilon_{\Delta} \mu_i}{1 + \varepsilon_{\Delta}} \underline{\underline{AS}}_{ve} + \frac{\Delta \lambda_p}{\tau_0} \underline{\underline{AMU}} \quad \text{or} \quad \underline{\underline{W}}^{-1} = \underline{\underline{I}} + \frac{\Delta \lambda_p}{\tau_0} \underline{\underline{AMU}}$$

$\underline{\underline{A}}$, $\underline{\underline{Y}}$ and $\underline{\underline{U}}$ being given by Eqs. (73)–(75) respectively. The unknown multiplier $\Delta \lambda_p$ is determined by solving the non-linear equation $f_p(n+1 \hat{\underline{\sigma}}, n+1 \underline{X}) = \bar{f}_p(\Delta \lambda_p) = 0$ where $n+1 \underline{X}$ is defined by Eq. (74).

The optimal choice of ζ may depend on the nature of the problem under consideration [16]. When large strain increments are considered, the fully implicit method corresponding to $\zeta = 1$ is probably optimal. On the other hand, in problems where strain increments remain small, the choice $\zeta = 0.5$ may yield improved accuracy with respect to the fully implicit procedure.

4.4.3. Viscoplastic correction

If a viscoplastic correction is necessary, it is performed by using in the general case:

$$n+1 \hat{\underline{\sigma}} = \underline{\underline{Q}}^\zeta \left\{ \overbrace{\left[\underline{\underline{I}} - (1 - \zeta) \left(\sum_i \frac{\varepsilon_{\Delta} \mu_i}{1 + \varepsilon_{\Delta} \zeta} \right) \underline{\underline{AS}}_{ve} \right] n\hat{\underline{\sigma}} + \underline{\underline{A}}\Delta \underline{\varepsilon} + \underline{\underline{A}} \sum_i \frac{\varepsilon_{\Delta}}{1 + \varepsilon_{\Delta} \zeta} n \underline{\underline{\zeta}}_i}^{\underline{\Psi}} - \Delta t \frac{n \dot{\lambda}_{vp}}{(n \dot{\lambda}_{vp}/K)^{1/N} + \tau_0}} \right. \\ \left. \times (1 - \zeta) \underline{\underline{AM}} \underline{\underline{I}} - \delta_3 \Delta t \frac{n+1 \dot{\lambda}_{vp}}{(n+1 \dot{\lambda}_{vp}/K)^{1/N} + \tau_0} \zeta \underline{\underline{Z}}^\zeta \underline{\underline{M}} \right) n(\hat{\underline{\sigma}} - \underline{X}_3) + \Delta t \frac{n+1 \dot{\lambda}_{vp}}{(n+1 \dot{\lambda}_{vp}/K)^{1/N} + \tau_0} \zeta \underline{\underline{AMZ}}^\zeta n\underline{X}_3 \left. \right\} \quad (86)$$

with:

$$\underline{\underline{Q}}^\zeta = \underline{\underline{I}} + \zeta \overbrace{\left(\sum_i \frac{\varepsilon_{\Delta} \mu_i}{1 + \varepsilon_{\Delta} \zeta} \right) \underline{\underline{AS}}_{ve} + \Delta t \frac{n+1 \dot{\lambda}_{vp}}{(n+1 \dot{\lambda}_{vp}/K)^{1/N} + \tau_0} \zeta \underline{\underline{AMV}}^\zeta}^{\underline{\underline{P}}}; \\ \underline{\underline{V}}^\zeta = \underline{\underline{I}} - \delta_3 \Delta t \frac{n+1 \dot{\lambda}_{vp}}{(n+1 \dot{\lambda}_{vp}/K)^{1/N} + \tau_0} \zeta \underline{\underline{Z}}^\zeta \underline{\underline{M}}; \\ \underline{\underline{Z}}^\zeta = \underline{\underline{I}} + \delta_3 \Delta t \frac{n+1 \dot{\lambda}_{vp}}{(n+1 \dot{\lambda}_{vp}/K)^{1/N} + \tau_0} \zeta \underline{\underline{M}} \quad (87)$$

for the generalised trapezoidal scheme (Eqs. (40) and (65)), $n+1 \dot{\lambda}_{vp}$ being determined by enforcing the ‘‘dynamic’’ yield condition (Eq. (31), see also Eq. (67)) at the end of the time step i.e.

$$f_{vp}^{\text{dyn}}(n+1 \hat{\underline{\sigma}}, n+1 \underline{X}_3; n+1 \dot{\lambda}_{vp}) = \bar{f}_{vp}^{\text{dyn}}(n+1 \dot{\lambda}_{vp}) = n+1 \overline{(\hat{\underline{\sigma}} - \underline{X}_3)} - \tau_0 - \left(\frac{n+1 \dot{\lambda}_{vp}}{K} \right)^{1/N} = 0 \quad (88)$$

where:

$${}_{n+1}\underline{X}_3 = \underline{Z}^\varsigma \left[{}_n\underline{X}_3 + \delta_3 \Delta t \frac{{}_n\dot{\lambda}_{vp}}{({}_n\dot{\lambda}_{vp}/K)^{1/N} + \tau_0} (1 - \varsigma) \underline{M}_n (\hat{\underline{\sigma}} - \underline{X}_3) + \delta_3 \Delta t \frac{{}_{n+1}\dot{\lambda}_{vp}}{({}_{n+1}\dot{\lambda}_{vp}/K)^{1/N} + \tau_0} \varsigma \underline{M}_{n+1} \hat{\underline{\sigma}} \right] \quad (89)$$

or:

$${}_{n+1}\hat{\underline{\sigma}} = \underline{Q}^\varsigma \left\{ \overbrace{\left[\underline{I} - (1 - \varsigma) \left(\sum_i \frac{\varepsilon_{\Delta} \mu_i}{1 + \varepsilon_{\Delta} \varsigma} \right) \underline{AS}_{ve} \right]}^{\underline{P}} \right] {}_n\hat{\underline{\sigma}} + \underline{A} \Delta \underline{\varepsilon} + \underline{A} \sum_i \frac{\varepsilon_{\Delta}}{1 + \varepsilon_{\Delta} \varsigma} {}_n\zeta_i - \Delta t \frac{{}_{n+\varsigma}\dot{\lambda}_{vp}}{({}_{n+\varsigma}\dot{\lambda}_{vp}/K)^{1/N} + \tau_0} \underline{AM} \right. \\ \left. \times \left[(1 - \varsigma) \underline{I} - \delta_3 \Delta t \frac{{}_{n+\varsigma}\dot{\lambda}_{vp}}{({}_{n+\varsigma}\dot{\lambda}_{vp}/K)^{1/N} + \tau_0} \varsigma \underline{Z}^\varsigma \underline{M} \right] ({}_{n+1}\hat{\underline{\sigma}} - \underline{X}_3) - \varsigma \underline{Z}^\varsigma {}_n\underline{X}_3 \right] \quad (90)$$

with:

$$(\underline{Q}^\varsigma)^{-1} = \underline{I} + \varsigma \overbrace{\left(\sum_i \frac{\varepsilon_{\Delta} \mu_i}{1 + \varepsilon_{\Delta} \varsigma} \right) \underline{AS}_{ve}}^{\underline{P}} + \Delta t \frac{{}_{n+\varsigma}\dot{\lambda}_{vp}}{({}_{n+\varsigma}\dot{\lambda}_{vp}/K)^{1/N} + \tau_0} \varsigma \underline{AMV}^\varsigma; \quad (91)$$

$$\underline{V}^\varsigma = \underline{I} - \delta_3 \Delta t \frac{{}_{n+\varsigma}\dot{\lambda}_{vp}}{({}_{n+\varsigma}\dot{\lambda}_{vp}/K)^{1/N} + \tau_0} \varsigma \underline{Z}^\varsigma \underline{M};$$

$$(\underline{Z}^\varsigma)^{-1} = \underline{I} + \delta_3 \Delta t \frac{{}_{n+\varsigma}\dot{\lambda}_{vp}}{({}_{n+\varsigma}\dot{\lambda}_{vp}/K)^{1/N} + \tau_0} \varsigma \underline{M}$$

for the generalised mid-point scheme (Eqs. (40) and (66)), ${}_{n+\varsigma}\dot{\lambda}_{vp}$ being determined by enforcing the ‘‘dynamic’’ yield condition at the intermediate time $t_{n+\varsigma}$ i.e. $({}_{n+\varsigma}(\cdot) = (1 - \varsigma)({}_n(\cdot) + \varsigma({}_{n+1}(\cdot)))$

$$f_{vp}^{\text{dyn}}({}_{n+\varsigma}\hat{\underline{\sigma}}; {}_{n+\varsigma}\underline{X}_3; {}_{n+\varsigma}\dot{\lambda}_{vp}) = \bar{f}_{vp}^{\text{dyn}}({}_{n+\varsigma}\dot{\lambda}_{vp}) = {}_{n+\varsigma}(\overline{({}_n\hat{\underline{\sigma}} - \underline{X}_3)}) - \tau_0 - \left(\frac{{}_{n+\varsigma}\dot{\lambda}_{vp}}{K} \right)^{1/N} = 0 \quad (92)$$

where:

$${}_{n+\varsigma}\underline{X}_3 = [(1 - \varsigma)\underline{I} + \varsigma \underline{Z}^\varsigma] {}_n\underline{X}_3 + \varsigma \underline{Z}^\varsigma \left\{ \delta_3 \Delta t \frac{{}_{n+\varsigma}\dot{\lambda}_{vp}}{({}_{n+\varsigma}\dot{\lambda}_{vp}/K)^{1/N} + \tau_0} [(1 - \varsigma) \underline{M}_n (\hat{\underline{\sigma}} - \underline{X}_3) + \varsigma \underline{M}_{n+1} \hat{\underline{\sigma}}] \right\} \quad (93)$$

For a creep behaviour (Section 4.1.3) some of these relations are simplified by using the trial stresses ${}_{n+1}\hat{\underline{\sigma}}^{\text{trial}}$ (Eq. (63)) as a substitute for \underline{P} in Eqs. (86) and (90), and by cancelling \underline{P} in Eqs. (87) and (91).

4.4.3.1. Local iterative solution procedure. The unknowns ${}_{n+1}\dot{\lambda}_{vp}$ and ${}_{n+\varsigma}\dot{\lambda}_{vp}$ being determined by enforcing the ‘‘dynamic’’ yield condition at the end of the time step and at the intermediate time $t_{n+\varsigma}$ for the generalised trapezoidal and mid-point schemes respectively, highly non-linear problems have to be solved and the use of an advanced numerical technique such as a line-search method [26,27] is greatly recommended to produce a robust solution algorithm since, for the considered problems, the classical Newton’s iterative scheme often fails.

A line-search method is an iterative method which guide the solution towards convergence by adjustment of a scalar multiplier η such as:

$${}_{n+\varsigma}\dot{\lambda}_{vp} = {}_{n+\varsigma}\dot{\lambda}_{vp}^0 + \eta \Delta^0; \quad \Delta^0 = - \frac{\bar{f}_{vp}^{\text{dyn}}({}_{n+\varsigma}\dot{\lambda}_{vp}^0)}{d\bar{f}_{vp}^{\text{dyn}}({}_{n+\varsigma}\dot{\lambda}_{vp}^0)}; \quad d\bar{f}_{vp}^{\text{dyn}}({}_{n+\varsigma}\dot{\lambda}_{vp}^0) = \left. \frac{d\bar{f}_{vp}^{\text{dyn}}({}_{n+\varsigma}\dot{\lambda}_{vp})}{d{}_{n+\varsigma}\dot{\lambda}_{vp}} \right|_{{}_{n+\varsigma}\dot{\lambda}_{vp}^0} \quad (94)$$

${}_{n+\varsigma}\dot{\lambda}_{vp}^0$ represents the previous convergent solution. As $\bar{f}_{vp}^{\text{dyn}}$ can be undefined at the origin, a dichotomy method is used to allow the iterative process initiation for the first viscoplastic increment.

Since a perturbation $\delta\eta$ of η induces a perturbation $\delta{}_{n+\varsigma}\dot{\lambda}_{vo}$ of ${}_{n+\varsigma}\dot{\lambda}_{vo}$ i.e.

$${}_{n+\varsigma}\dot{\lambda}_{vo} + \delta{}_{n+\varsigma}\dot{\lambda}_{vo} = {}_{n+\varsigma}\dot{\lambda}_{vo}^0 + (\eta + \delta\eta) \Delta^0 \quad (95)$$

the original problem $\dot{\bar{f}}_{vp}^{dyn}(n+\zeta\lambda_{vp}) = 0$ can be replaced by the equivalent one $\bar{g}(\eta) = 0$. In practice, it is unprofitable to determine η by solving $\bar{g}(\eta) = 0$, it is better to minimise the ratio $|r(\eta)| = |\bar{g}(\eta)/\bar{g}(0)|$ (slack line search). Hence, while $|r(\eta)| \geq 10^{-10}$ (user tolerance), η is updated by using:

$$\eta^{i+1} = \eta^i \left(\frac{\bar{g}(0)}{\bar{g}(0) - \bar{g}(\eta^i)} \right) \quad (96)$$

if $r(\eta) < 0$, else, by using an extrapolation which has to be limited by an amplification coefficient (see [26] for more details).

4.4.3.2. Comparative accuracy analysis. Optimal algorithms being obtained for $\zeta = 1/2$, an accuracy analysis is performed hereafter in order to compare the generalised trapezoidal and mid-point rules. These schemes lead to two different procedures in viscoplasticity for $\zeta \in]0, 1[$.

Considering an elasto-viscoplastic behaviour, such an analysis concerns a single loading direction since, using Kirchhoff shell elements, the viscoplastic flow occurs only by shearing in the plane (\vec{x}_1, \vec{x}_2) . The algorithmic shear solutions $\hat{\sigma}_{12}$ and $(X_3)_{12}$ (see boxes 4 and 5) can then be compared to the analytical ones ${}^{Ref}\hat{\sigma}_{12}(t)$ and ${}^{Ref}(X_3)_{12}(t)$ obtained by solving the following differential system:

$$\begin{cases} {}^{Ref}\dot{\hat{\sigma}}_{12} = A_{44}\dot{\gamma}_{12} - A_{44}K [{}^{Ref}\hat{\sigma}_{12} - {}^{Ref}(X_3)_{12} - \tau_0]^N \\ {}^{Ref}(\dot{X}_3)_{12} = \delta_3 K [{}^{Ref}\hat{\sigma}_{12} - {}^{Ref}(X_3)_{12} - \tau_0]^N; \\ \gamma_{12} = kt \end{cases} \quad (97)$$

with the initial conditions: ${}^{Ref}\hat{\sigma}_{12}(t_i) = \tau_0$ and ${}^{Ref}(X_3)_{12}(t_i) = 0$; $t_i = \tau_0/kA_{44}$, corresponding at the outset of the viscoplastic flow, k represents a constant shear strain rate.

Figs. 2–4 show the obtained results for a total shear value $\gamma_{12} = 0.05$, divided into 10 equal increments ($\Delta\gamma_{12} = 0.005$). The considered sample is a square plate 1×1 mm², composed of a single layer orientated along the shear direction. Its material properties are [28]: $A_{44} = G_{12} = 9300$ MPa, $\delta_3 = 7366$ MPa, $K = 2.5710^{-11}$ and $\tau_0 = 13.37$ MPa. Four values are considered for the rate-sensitivity parameter N which affects the non-linearity of the problem to be solved (Eq. (88) or Eq. (92)): $N = 1, 3.93$ (identified for this material), 5 and 10.

Fig. 2 shows the relative errors on the algorithmic solutions for various loading rates in the case $\zeta = 1$ (the trapezoidal and mid-point rules lead to a same procedure in this case). When 1% error can be reached for $\hat{\sigma}_{12}$, more than 25% error are recorded for $(X_3)_{12}$. In each case, the maximum error i.e. its value and the corresponding rates, strongly

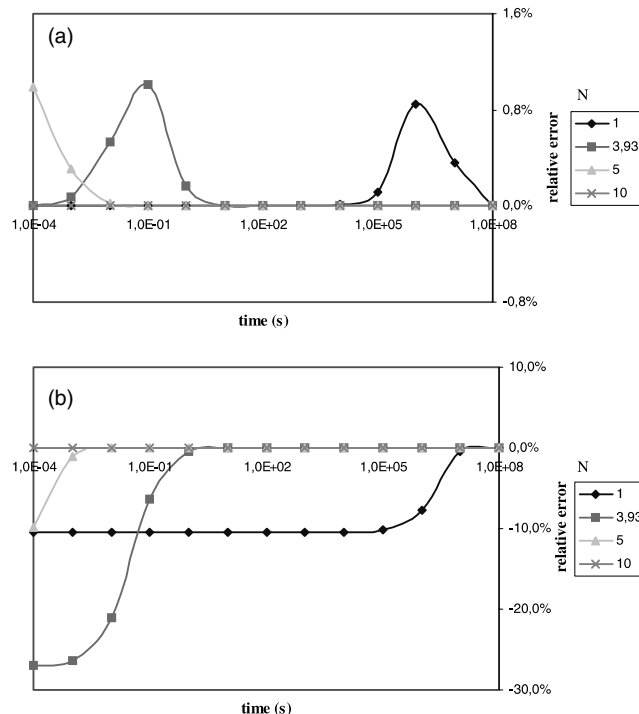


Fig. 2. Relative errors on the algorithmic solutions for a fully implicit integration: (a) $\hat{\sigma}_{12}$ and (b) $(X_3)_{12}$.

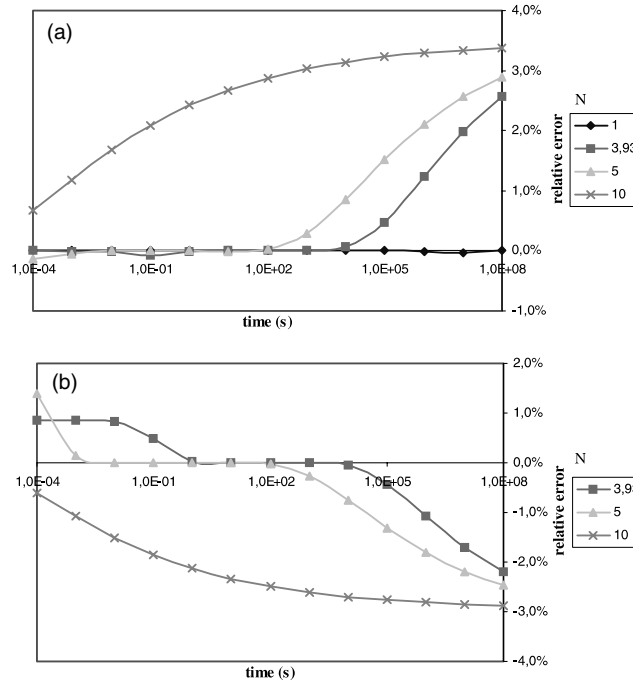


Fig. 3. Relative errors on the algorithmic solutions for the generalised mid-point rule in the case $\zeta = 0.5$: (a) $\hat{\sigma}_{12}$ and (b) $(X_3)_{12}$.

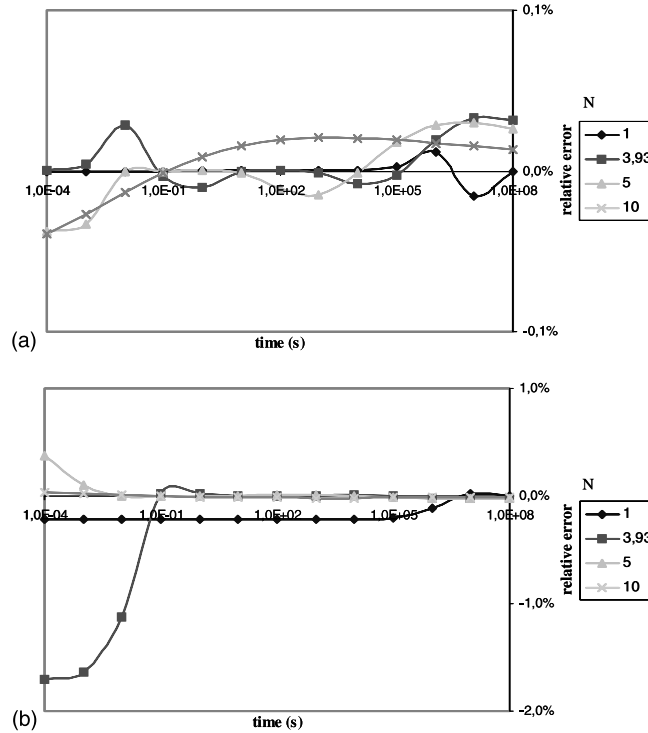


Fig. 4. Relative errors on the algorithmic solutions for the generalised trapezoidal rule in the case $\zeta = 0.5$: (a) $\hat{\sigma}_{12}$ and (b) $(X_3)_{12}$.

depends on the rate-sensitivity parameter N . The greater the N value, the more important error at high loading rates, the minimum error is obtained for $N = 10$ for the considered rate range.

Fig. 3 shows the relative errors on the algorithmic solutions obtained for various loading rates by using the generalised mid-point rule in the case $\zeta = 1/2$. When the error on $\hat{\sigma}_{12}$ slightly increases ($\approx 3.5\%$), the one on $(X_3)_{12}$ appreciably decreases ($\approx -3\%$). In each case, a same effect of the rate-sensitivity parameter N is observed. The greater the

N value, the more important error at low loading rates, the maximum error is obtained for $N = 10$ for the considered rate range.

Fig. 4 shows the relative errors on the algorithmic solutions obtained for various loading rates by using the generalised trapezoidal rule in the case $\zeta = 1/2$. When the error on $\hat{\sigma}_{12}$ becomes negligible ($\approx 0.03\%$), the one on $(X_3)_{12}$ reaches a maximum of $\approx -1.5\%$. In this last case, the effect of the rate-sensitivity parameter N is comparable to the one observed for $\zeta = 1$.

The development of state variables integration algorithms with improved performance has received considerable attention in the recent literature on computational viscoplasticity. In this, the fully implicit method ($\zeta = 1$) has been particularly emphasised, mainly because of its simplicity and wider range of applicability. Nevertheless, in the present case, this method needs a great number of increments to converge towards a satisfactory algorithmic solutions in comparison with the semi-implicit ($\zeta = 1/2$) generalised trapezoidal scheme which seems to be the more interesting approach (but for which the B-stability remains an open problem). The rate-sensitivity parameter effects that depend on the used algorithm are appreciably attenuated by this approach.

4.4.4. Plastic-viscoplastic correction

If a plastic-viscoplastic correction is necessary, it can be performed by using Eq. (78) or Eq. (79), for example, in the case of a fully implicit integration. The unknowns $\Delta\lambda_p$ and ${}_{n+1}\dot{\lambda}_{vp}$ derive from the yield conditions:

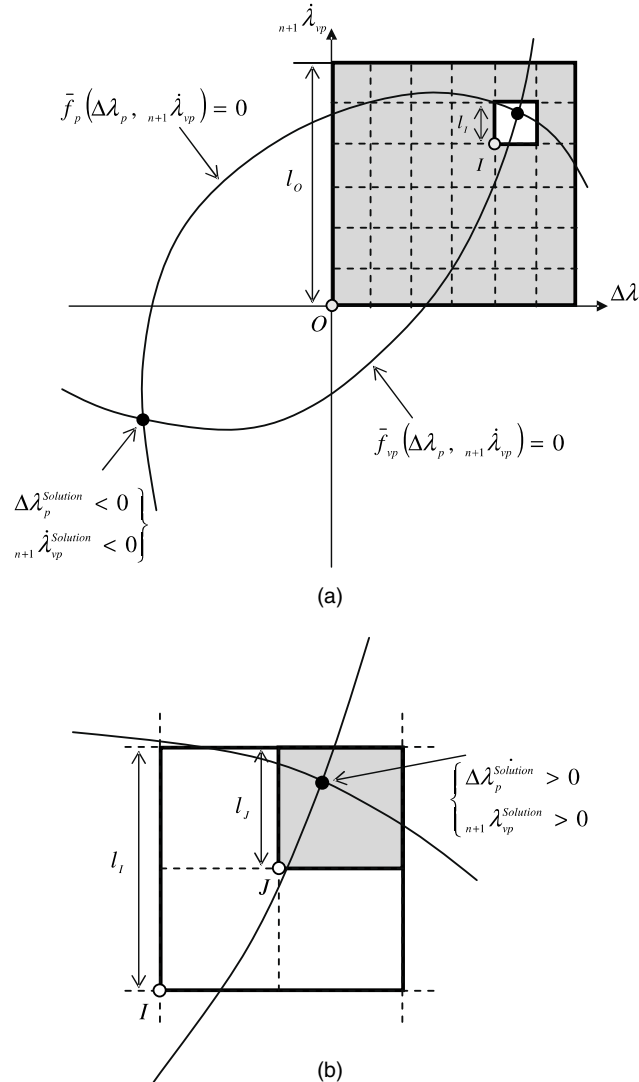


Fig. 5. (a) Original and (b) refined search of simultaneous zero-crossing curves of both functions \bar{f}_p and \bar{f}_{vp} in the case of multi-modal problems.

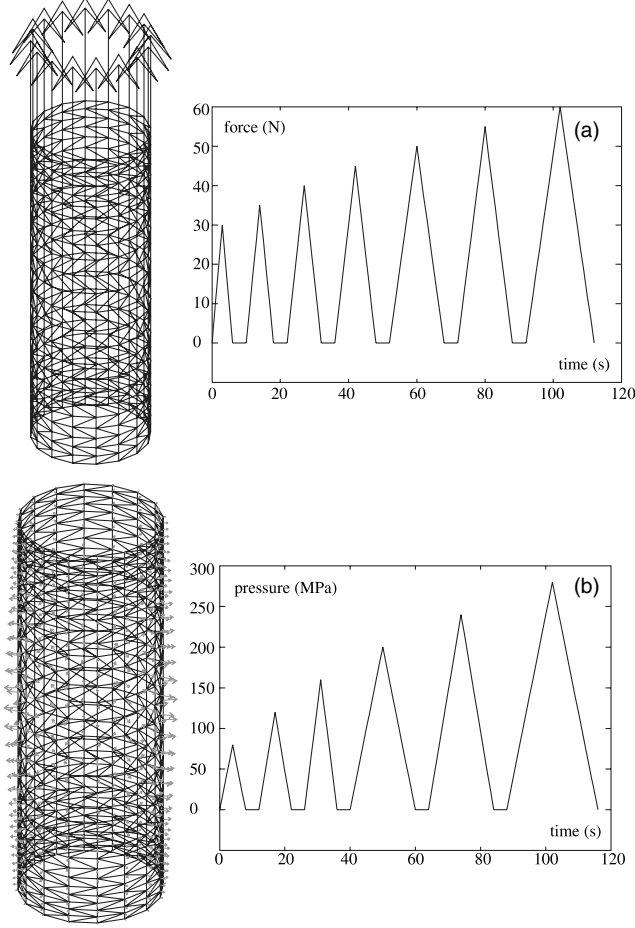


Fig. 6. Numerical models and loading cycles in (a) pure traction and (b) pure internal pressure.

$$f_p(n_{+1}\hat{\underline{\underline{\sigma}}}, n_{+1}\underline{\underline{X}}) = \bar{f}_p(\Delta\lambda_p, n_{+1}\dot{\lambda}_{vp}) = 0, \quad f_{vp}^{dyn}(n_{+1}\hat{\underline{\underline{\sigma}}}, n_{+1}\underline{\underline{X}}_3; n_{+1}\dot{\lambda}_{vp}) = \bar{f}_{vp}(\Delta\lambda_p, n_{+1}\dot{\lambda}_{vp}) = 0 \quad (98)$$

$n_{+1}\underline{\underline{X}}$ and $n_{+1}\underline{\underline{X}}_3$ being given by Eqs. (74) and (76) respectively.

It has been verified that such a coupled problem can be multi-modal (see Fig. 5). Hence, in order to assure the determination of positive solutions, a grid-search method [29] is used in association with the classical Newton's iterative scheme to define available starting values (see box 6). A first search in a positive region of dimension two with lower left co-ordinates (0, 0), gives lower left co-ordinates and dimension of squares where there are simultaneous zero-crossing curves of both functions $\bar{f}_p(\Delta\lambda_p, n_{+1}\dot{\lambda}_{vp})$ and $\bar{f}_{vp}(\Delta\lambda_p, n_{+1}\dot{\lambda}_{vp})$ (zero-crossing curves intersection give the solutions of the non-linear system, Eq. (98)). To keep track of the squares of various sizes that are to be searched further by refinement until there is a final set of squares having crossing of dimension less than the user entered precision, software stack ⁴ is used. In practice, lower left co-ordinates found in the original search are sufficient to efficiently initiate the Newton's iterative scheme.

4.4.5. (Visco)elasto-(visco)plastic prediction–damage correction

The final state of the material is obtained after a (visco)elasto-(visco)plastic prediction where the degradation of the material is stopped:

$$n_{+1}\underline{\underline{\sigma}}^{trial} = \underline{\underline{L}}_{n+1}\hat{\underline{\underline{\sigma}}}; \quad \underline{\underline{L}}^{-1} = \underline{\underline{I}} + \underline{\underline{A}}\underline{\underline{H}}(nD) \quad (99)$$

If the damage yield condition is not violated, the current step is evaluated to be (visco)elasto-(visco)plastic, the trial stresses $n_{+1}\underline{\underline{\sigma}}^{trial}$ are admissible and are accepted as final stresses. Otherwise, a damage correction is necessary and is

⁴ The stack is just a list of the co-ordinates and dimension of each of the squares to be searched further.

performed by updating the damage variable which is expressed in term of the unknown damage multiplier $\Delta\lambda_d$ (see [1] for more details).

5. Algorithmic tangent operator

The necessity to take account of the numerical integration procedure into the evaluation of the tangent operator $\underline{\underline{B}}$ such as:

$$d_{[n+1]\underline{\underline{\sigma}}} = \underline{\underline{B}}d_{[n+1]\underline{\underline{\varepsilon}}} \tag{100}$$

has been first outlined in [30] and in [31,32] a consistent tangent operator has been effectively defined for elasto-plastic models in order to guarantee the asymptotically quadratic rate of convergence which characterises the full Newton–Raphson algorithm. By replacing the consistency condition classically adopted in plasticity with an analogous relation based on the “dynamic” yield function (Eq. (31)), such an operator has been recently generalised for viscoplastic models [12,15].

As the proposed theory herein encompasses a viscoelastic behaviour (Eq. (40) or Eq. (63)), the determination of a consistent tangent operator is non-trivial. The numerical perturbation technique [33–35] becomes then a very interesting alternative to evaluate $\underline{\underline{B}}$. This technique consists of the following steps:

- (i) Each component of the strain increment $\Delta\underline{\underline{\varepsilon}}$ is successively perturbed: $\Delta\underline{\underline{\varepsilon}}^k = \Delta\underline{\underline{\varepsilon}} + \delta^k$
- (ii) Evaluate the corresponding effective stress state ${}_{n+1}\hat{\underline{\underline{\sigma}}}^k$ following the algorithm in box 7

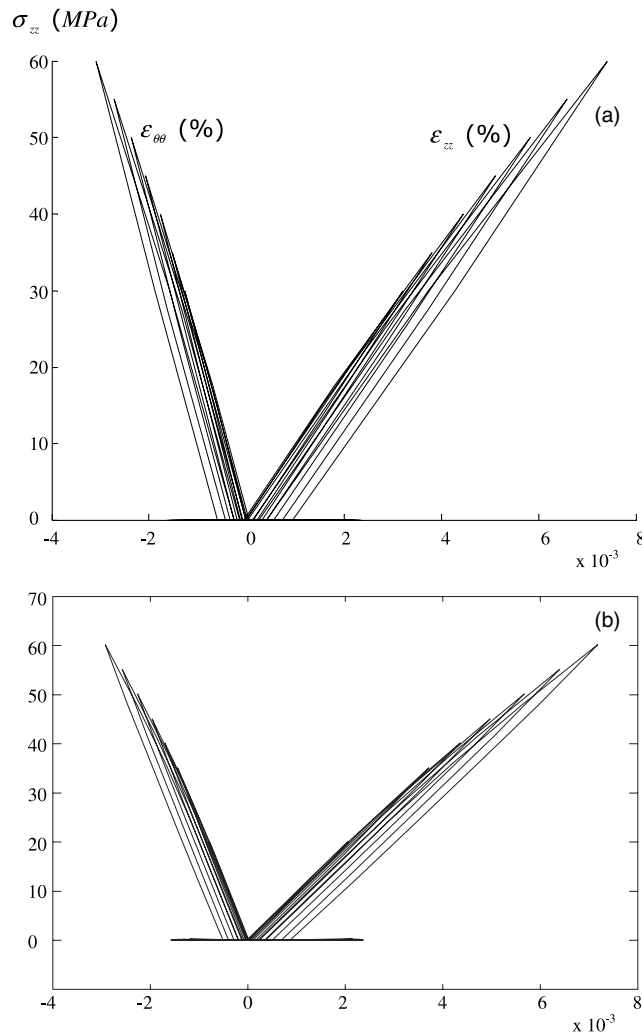


Fig. 7. (a) Semi-analytical and (b) numerical results in pure traction.

- (iii) Compute the effective stress perturbation: $\delta \hat{\underline{\sigma}}^k = {}_{n+1} \hat{\underline{\sigma}}^k - {}_n \hat{\underline{\sigma}}$
- (iv) Compute the column vector: $\underline{C}^k = \delta \hat{\underline{\sigma}}^k / \delta^k$
- (v) Compose the (4×4) matrix $\hat{\underline{C}}^{v-ep} = [\underline{C}^1, \underline{C}^2, \underline{C}^3, \underline{C}^4]$
- (vi) Reduce $\hat{\underline{C}}^{v-ep}$ to a (3×3) matrix by using the relationship between $d\varepsilon_{33}$, $d\varepsilon_{22}$ and $d\varepsilon_{33}$ (Eq. (83))
- (vii) Compute

$$\underline{B} = \left[\underline{L} - \frac{\underline{L} \underline{A} \underline{H}' {}_{n+1} \underline{\sigma} ({}_{n+1} \underline{\sigma} \underline{H}' \underline{L})}{{}_{n+1} \underline{\sigma} (\underline{H}' \underline{L} \underline{A} \underline{H}' - \underline{H}'') {}_{n+1} \underline{\sigma} + y'} \right] \hat{\underline{C}}^{v-ep}; \quad \underline{H}' = \frac{\partial \underline{H}}{\partial D}, \quad \underline{H}'' = \frac{1}{2} \frac{\partial^2 \underline{H}}{\partial D^2}$$

(see [1, Section 5])

This tangent operator is redefined in Appendix B when a viscous regularisation is used to correct ill-posed standard boundary value problems for which finite element computations exhibit spurious mesh sensitivity when the mesh is refined to vanishing size.

6. Applications

In this section, the comparison between semi-analytical results obtained with the classical laminate theory, suitably extended for non-linear analysis [28], and numerical results obtained through the implementation of the proposed modelling into the finite element code CASTEM2000[®], is investigated.

The considered tests concern a $[+55, -55]_6$ layer tube (length = 180 mm, mid-radius = 31 mm, thickness = 2 mm). The following material constants have been used:

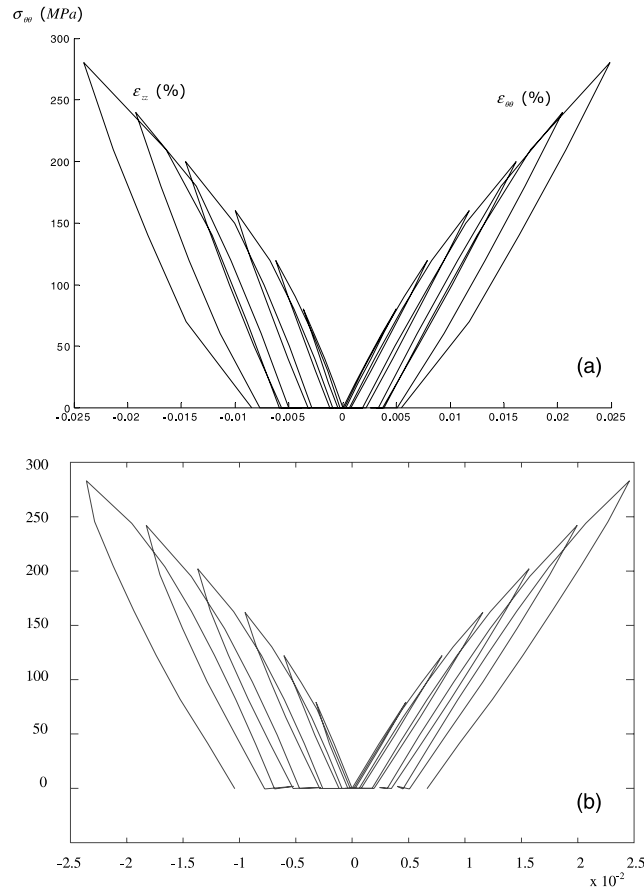


Fig. 8. (a) Semi-analytical and (b) numerical results in pure internal pressure.

$E_1 = 38910$ MPa, $E_2 = 9900$ MPa, $G_{12} = 3799$ MPa, $\nu_{12} = 0.25$, $\nu_{23} = 0.2$, $n_0 = 9.03$, $n_b = 30$,
 $n_c = 7.84$, $\beta_t = 1.74$, $\beta_{tt} = 1$, $\beta_{lt} = 0.85$, $Y_c = 0.0027$ MPa, $q = 1.246$ MPa, $p = 0.816$,
 $\tau_0 = 14.23$ MPa, $\delta_1 = 25000$ MPa, $\delta_2 = 1800$ MPa, $\gamma_1 = 900$, $K = 2.2 \times 10^{11}$ [MPa]^{-N}s, $N = 1.75$,
 $\delta_3 = 12000$ MPa

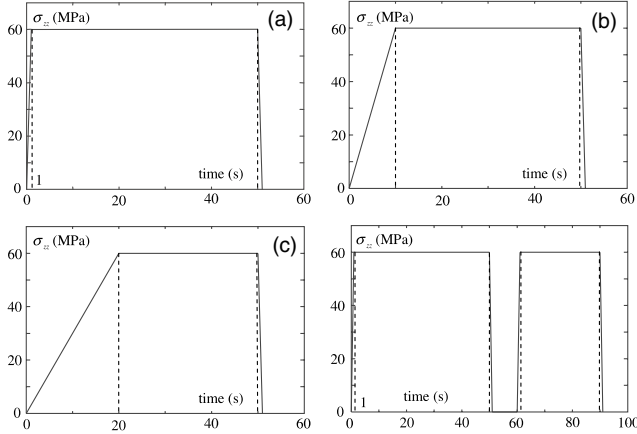


Fig. 9. Creep loading conditions.

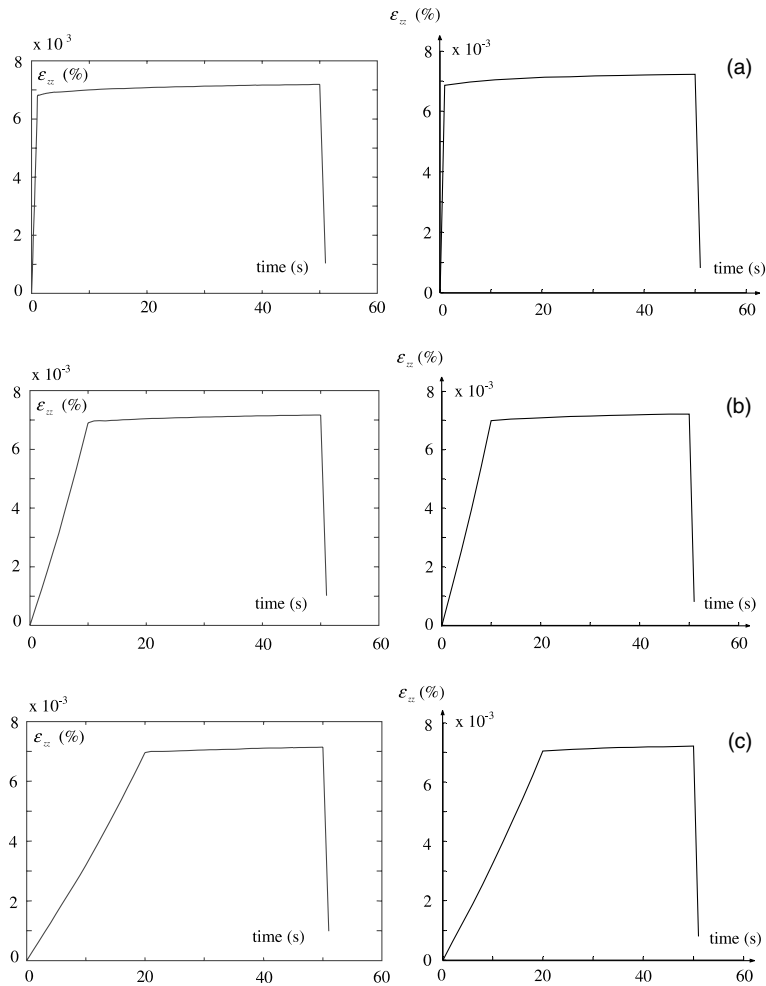


Fig. 10. Semi-analytical (right hand side) and numerical (left hand side) creep strains.

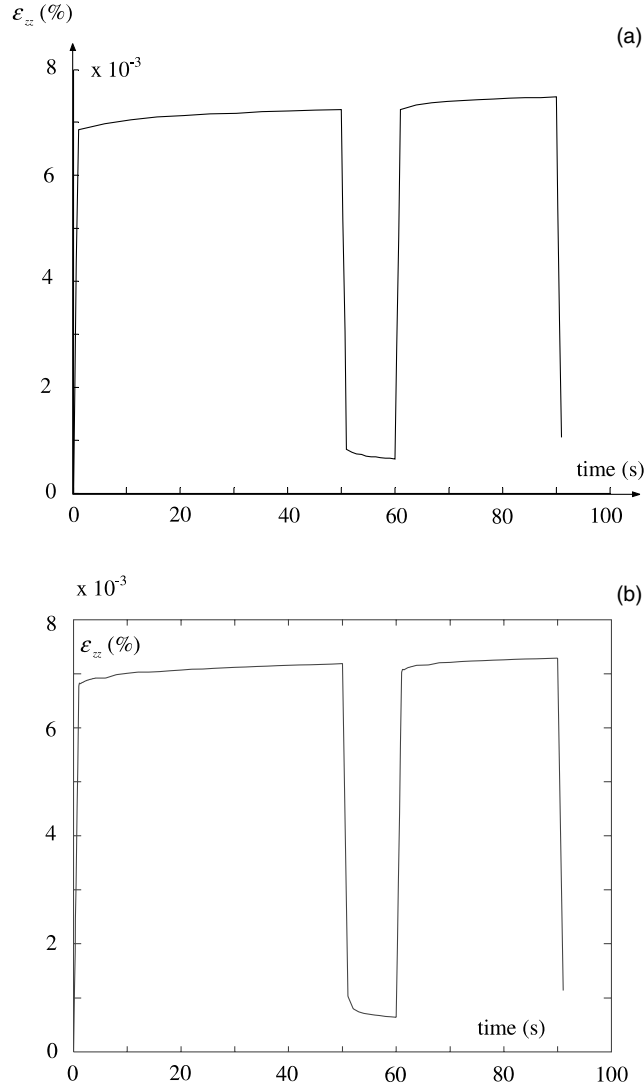


Fig. 11. Semi-analytical (a) and numerical (b) creep strains.

The used meshing and the progressive repeated loading conditions in pure traction and in pure internal pressure are shown Fig. 6. The pure traction test has been performed by using 768 elements and 55 equal increments when 640 elements and 63 equal increments have been used in pure internal pressure. For these two tests, a good agreement is obtained (see Figs. 7 and 8) between the finite element results and the semi-analytical ones. Very satisfactory results have also been obtained (see Figs. 10 and 11) in the case of creep behaviours in pure traction (see Fig. 9).

7. Conclusion

In addition to the time-independent behaviour model presented in the first part of this article within the context of a meso–macro approach, a viscous one is proposed herein to account for creep strains at the layer level. This model consists of a viscoelastic component based on a relaxation times triangular spectrum and of a viscoplastic component based on a generalised Norton-type dissipation potential integrating the elastic domain concept. In order to allow a same treatment of viscoplastic and classical plastic problems, a “dynamic” yield function is incorporated in the usual viscous format. Using the well-known generalised trapezoidal and mid-point integration rules, second order accurate and B-stable state computation algorithms are proposed in association with reliable local iterative solution procedures

within a multi-step predictor–corrector scheme. Considering an elasto-viscoplastic behaviour, a comparative accuracy analysis shows that the generalised trapezoidal rule, for which the B-stability remains, to our knowledge, an open question, is more accurate than the generalised mid-point rule. Since the viscoelasticity renders non-trivial the determination of a consistent tangent operator with the proposed state computation algorithms, a perturbation technique is suggested to derive an algorithmic tangent operator. This operator can be easily reformulated when a visco-damage model is considered to overcome localisation problems.

Following the methodology proposed in the first part of this article, the inter-laminar stresses can be evaluated taking account of the viscous behaviours.

In order to compare the proposed modelling with experimental results, a reliable parameters identification method must be developed. In a forthcoming paper, an inverse technique using local methods associated with a genetic algorithm will be presented and applied to multi-axial tests. Moreover, the proposed model will be complemented in order to account for micro-cracks closure–opening effects using a strain criterion.

Appendix A. Viscoplastic numerical models accuracy and stability analysis

A.1. Accuracy analysis

As done Section 4.1.1, an accuracy analysis of the obtained viscoplastic numerical models (Eqs. (64)–(69)) can be performed by comparing algorithmic and exact stresses using the Taylor series expansion expressed by Eqs. (41) and (43).

For the generalised trapezoidal and mid-point rules, the stresses first and second time derivatives are:

$$\begin{aligned} \frac{d}{d\Delta t} \left({}_{n+1}\hat{\underline{\sigma}} \right) \Big|_{\Delta t=0} &= \underline{\underline{A}}_n \dot{\underline{\underline{\sigma}}} - \underline{\underline{A}} \left[\frac{{}_n\dot{\lambda}_{vp}}{({}_n\dot{\lambda}_{vp}/K)^{1/N} + \tau_0} \underline{\underline{M}}({}_n\hat{\underline{\sigma}} - {}_n\underline{\underline{X}}_3) \right] \\ \frac{d^2}{d\Delta t^2} \left({}_{n+1}\hat{\underline{\sigma}} \right) \Big|_{\Delta t=0} &= \underline{\underline{A}}_n \ddot{\underline{\underline{\sigma}}} - 2\zeta \underline{\underline{A}} \left\{ \frac{{}_n\ddot{\lambda}_{vp} \left[({}_n\dot{\lambda}_{vp}/K)^{1/N} \left(1 - \frac{1}{N}\right) + \tau_0 \right]}{\left[({}_n\dot{\lambda}_{vp}/K)^{1/N} + \tau_0 \right]^2} \underline{\underline{M}}({}_n\hat{\underline{\sigma}} - {}_n\underline{\underline{X}}_3) + \frac{{}_n\dot{\lambda}_{vp}}{({}_n\dot{\lambda}_{vp}/K)^{1/N} + \tau_0} \underline{\underline{M}}({}_n\dot{\underline{\underline{\sigma}}} - {}_n\dot{\underline{\underline{X}}}_3) \right\} \end{aligned} \quad (\text{A.1})$$

Compared to the exact ones (see box 2):

$$\begin{aligned} {}_n\hat{\underline{\underline{\sigma}}} &= \underline{\underline{A}}_n \dot{\underline{\underline{\sigma}}} - \underline{\underline{A}} \left[\frac{{}_n\dot{\lambda}_{vp}}{({}_n\dot{\lambda}_{vp}/K)^{1/N} + \tau_0} \underline{\underline{M}}({}_n\hat{\underline{\sigma}} - {}_n\underline{\underline{X}}_3) \right] \\ {}_n\ddot{\underline{\underline{\sigma}}} &= \underline{\underline{A}}_n \ddot{\underline{\underline{\sigma}}} - \underline{\underline{A}} \left\{ \frac{{}_n\ddot{\lambda}_{vp} \left[({}_n\dot{\lambda}_{vp}/K)^{1/N} \left(1 - \frac{1}{N}\right) + \tau_0 \right]}{\left[({}_n\dot{\lambda}_{vp}/K)^{1/N} + \tau_0 \right]^2} \underline{\underline{M}}({}_n\hat{\underline{\sigma}} - {}_n\underline{\underline{X}}_3) + \frac{{}_n\dot{\lambda}_{vp}}{({}_n\dot{\lambda}_{vp}/K)^{1/N} + \tau_0} \underline{\underline{M}}({}_n\dot{\underline{\underline{\sigma}}} - {}_n\dot{\underline{\underline{X}}}_3) \right\} \end{aligned} \quad (\text{A.2})$$

they show a second order accuracy for $\zeta = 1/2$ in the usual sense of the local truncation error.

A.2. Stability analysis

Consider the standard evolution problem given by Eq. (45) where:

$$\underline{\underline{\Sigma}} = \begin{pmatrix} \hat{\underline{\sigma}} \\ \underline{\underline{X}}_3 \end{pmatrix}, \quad \underline{\underline{E}} = \begin{pmatrix} \dot{\underline{\sigma}} \\ \underline{\underline{0}} \end{pmatrix}, \quad \underline{\underline{\Xi}} = \begin{pmatrix} \dot{\underline{\sigma}}^{vp} \\ -\dot{\underline{\underline{X}}}_3 \end{pmatrix} = \begin{pmatrix} \dot{\lambda}_{vp} \frac{\partial f_{vp}}{\partial \underline{\underline{\sigma}}} \\ \dot{\lambda}_{vp} \frac{\partial f_{vp}}{\partial \underline{\underline{X}}_3} \end{pmatrix}, \quad \underline{\underline{G}} = \begin{bmatrix} \underline{\underline{A}} & \underline{\underline{0}} \\ \underline{\underline{0}} & \delta_3 \underline{\underline{I}} \end{bmatrix} \quad (\text{A.3})$$

This problem is contractive relative to the norm $\|(\cdot)\|_G$ if:

$$\begin{aligned} \frac{d}{dt} \|\underline{\Sigma} - \underline{\Sigma}'\|_G^2 &= 2\dot{\lambda}_{vp} \left[\frac{\text{T}\partial f_{vp}}{\partial \hat{\underline{\sigma}}} \Big|_{\hat{\underline{\sigma}}, \underline{X}_3} (\hat{\underline{\sigma}} - \hat{\underline{\sigma}}') + \frac{\text{T}\partial f_{vp}}{\partial \underline{X}_3} \Big|_{\hat{\underline{\sigma}}, \underline{X}_3} (\underline{X}_3 - \underline{X}_3') \right] + 2\dot{\lambda}_{vp} \left[\frac{\text{T}\partial f_{vp}}{\partial \hat{\underline{\sigma}}} \Big|_{\hat{\underline{\sigma}}, \underline{X}_3} (\hat{\underline{\sigma}}' - \hat{\underline{\sigma}}) \right. \\ &\quad \left. + \frac{\text{T}\partial f_{vp}}{\partial \underline{X}_3} \Big|_{\hat{\underline{\sigma}}, \underline{X}_3} (\underline{X}_3' - \underline{X}_3) \right] \leq 0 \quad \forall t \end{aligned} \quad (\text{A.4})$$

f_{vp} (Eq. (28)) being a convex function, it verifies:

$$f_{vp}(\hat{\underline{\sigma}}, \underline{X}_3') - f_{vp}(\hat{\underline{\sigma}}, \underline{X}_3) \geq \frac{\text{T}\partial f_{vp}}{\partial \hat{\underline{\sigma}}} \Big|_{\hat{\underline{\sigma}}, \underline{X}_3} (\hat{\underline{\sigma}}' - \hat{\underline{\sigma}}) + \frac{\text{T}\partial f_{vp}}{\partial \underline{X}_3} \Big|_{\hat{\underline{\sigma}}, \underline{X}_3} (\underline{X}_3' - \underline{X}_3), \quad \forall [(\hat{\underline{\sigma}}, \underline{X}_3'), (\hat{\underline{\sigma}}, \underline{X}_3)] \quad (\text{A.5})$$

Hence:

$$\frac{d}{dt} \|\underline{\Sigma} - \underline{\Sigma}'\|_G^2 \leq 2\dot{\lambda}_{vp} [f_{vp}(\hat{\underline{\sigma}}, \underline{X}_3) - f_{vp}(\hat{\underline{\sigma}}, \underline{X}_3')] + 2\dot{\lambda}_{vp} [f_{vp}(\hat{\underline{\sigma}}, \underline{X}_3') - f_{vp}(\hat{\underline{\sigma}}, \underline{X}_3)] \quad (\text{A.6})$$

This inequality can be reformulated taking account of Eq. (31), so:

$$\begin{aligned} \frac{d}{dt} \|\underline{\Sigma} - \underline{\Sigma}'\|_G^2 &\leq 2\dot{\lambda}_{vp} \left[f_{vp}^{\text{dyn}}(\hat{\underline{\sigma}}, \underline{X}_3; \dot{\lambda}_{vp}) + \left(\frac{\dot{\lambda}_{vp}}{K} \right)^{1/N} - f_{vp}^{\text{dyn}}(\hat{\underline{\sigma}}, \underline{X}_3'; \dot{\lambda}_{vp}) - \left(\frac{\dot{\lambda}_{vp}}{K} \right)^{1/N} \right] + 2\dot{\lambda}_{vp} \left[f_{vp}^{\text{dyn}}(\hat{\underline{\sigma}}, \underline{X}_3'; \dot{\lambda}_{vp}) \right. \\ &\quad \left. + \left(\frac{\dot{\lambda}_{vp}}{K} \right)^{1/N} - f_{vp}^{\text{dyn}}(\hat{\underline{\sigma}}, \underline{X}_3; \dot{\lambda}_{vp}) - \frac{\dot{\lambda}_{vp}}{K} \right] \end{aligned} \quad (\text{A.7})$$

For $f_{vp}^{\text{dyn}}(\hat{\underline{\sigma}}, \underline{X}_3; \dot{\lambda}_{vp}) \leq 0$ and $f_{vp}^{\text{dyn}}(\hat{\underline{\sigma}}, \underline{X}_3'; \dot{\lambda}_{vp}) \leq 0$ i.e. $f_{vp}(\hat{\underline{\sigma}}, \underline{X}_3) \leq 0$ and $f_{vp}(\hat{\underline{\sigma}}, \underline{X}_3') \leq 0$, the contractivity property is verified since $\dot{\lambda}_{vp} = \dot{\lambda}_{vp}' = 0$. Otherwise, for $\dot{\lambda}_{vp} > 0$ and $\dot{\lambda}_{vp}' > 0$ (Eq. (31))

$$f_{vp}^{\text{dyn}}(\hat{\underline{\sigma}}, \underline{X}_3; \dot{\lambda}_{vp}) = f_{vp}^{\text{dyn}}(\hat{\underline{\sigma}}, \underline{X}_3'; \dot{\lambda}_{vp}') = 0 \quad (\text{A.8})$$

what leads to:

$$\frac{d}{dt} \|\underline{\Sigma} - \underline{\Sigma}'\|_G^2 \leq 2 \left[\left(\frac{\dot{\lambda}_{vp}}{K} \right)^{1/N} - \frac{\dot{\lambda}_{vp}}{K} \right] (\dot{\lambda}_{vp} - \dot{\lambda}_{vp}') \quad (\text{A.9})$$

$\dot{\lambda}_{vp}$ and $\dot{\lambda}_{vp}'$ being positive, it comes then immediately $\frac{d}{dt} \|\underline{\Sigma} - \underline{\Sigma}'\|_G^2 \leq 0$.

Established by using the properties of the ‘‘dynamic’’ yield function f_{vp}^{dyn} , this result extends the contractivity property obtained in [20] for a linear viscoplastic model of Perzyna type.

The algorithm obtained by using the mid-point scheme (Eqs. (64), (66), (67) and (69)) is said B-stable if the condition (Eq. (52)) is verified, the algorithmic solutions being given by:

$${}_{n+1}\underline{\Sigma} = {}_n\underline{\Sigma} + \underline{G}(\Delta \underline{E} - \Delta \underline{E}'), \quad {}_{n+1}\underline{\Sigma}' = {}_n\underline{\Sigma}' + \underline{G}(\Delta \underline{E}' - \Delta \underline{E}') \quad (\text{A.10})$$

where:

$$\Delta \underline{E} = \Delta t_{n+\zeta} \dot{\lambda}_{vp} \frac{\underline{M}({}_{n+\zeta}\hat{\underline{\sigma}} - {}_{n+\zeta}\underline{X}_3)}{({}_{n+\zeta}\hat{\underline{\sigma}} - {}_{n+\zeta}\underline{X}_3)} \begin{pmatrix} 1 \\ -1 \end{pmatrix} = \begin{pmatrix} \Delta t_{n+\zeta} \dot{\lambda}_{vp} \frac{\partial f_{vp}}{\partial \hat{\underline{\sigma}}} \Big|_{{}_{n+\zeta}\hat{\underline{\sigma}}, {}_{n+\zeta}\underline{X}_3} \\ \Delta t_{n+\zeta} \dot{\lambda}_{vp} \frac{\partial f_{vp}}{\partial \underline{X}_3} \Big|_{{}_{n+\zeta}\hat{\underline{\sigma}}, {}_{n+\zeta}\underline{X}_3} \end{pmatrix} \quad (\text{A.11})$$

Considering the relation (Eq. (57)) such as:

$$\begin{aligned} \|{}_{n+1}\underline{\Sigma} - {}_{n+1}\underline{\Sigma}'\|_G^2 - \|{}_n\underline{\Sigma} - {}_n\underline{\Sigma}'\|_G^2 &= 2{}^T_{n+\zeta}\underline{\Sigma}(\Delta \underline{E}' - \Delta \underline{E}) + 2{}^T_{n+\zeta}\underline{\Sigma}'(\Delta \underline{E} - \Delta \underline{E}') + (1 - 2\zeta) \left\| \underline{G}(\Delta \underline{E}' - \Delta \underline{E}) \right\|_G^2 \\ &= 2\Delta t_{n+\zeta} \dot{\lambda}_{vp} \left[\frac{\text{T}\partial f_{vp}}{\partial \hat{\underline{\sigma}}} \Big|_{{}_{n+\zeta}\hat{\underline{\sigma}}, {}_{n+\zeta}\underline{X}_3} ({}_{n+\zeta}\hat{\underline{\sigma}} - {}_{n+\zeta}\hat{\underline{\sigma}}') + \frac{\text{T}\partial f_{vp}}{\partial \underline{X}_3} \Big|_{{}_{n+\zeta}\hat{\underline{\sigma}}, {}_{n+\zeta}\underline{X}_3} ({}_{n+\zeta}\underline{X}_3 - {}_{n+\zeta}\underline{X}_3') \right] \\ &\quad + 2\Delta t_{n+\zeta} \dot{\lambda}_{vp} \left[\frac{\text{T}\partial f_{vp}}{\partial \hat{\underline{\sigma}}} \Big|_{{}_{n+\zeta}\hat{\underline{\sigma}}, {}_{n+\zeta}\underline{X}_3} ({}_{n+\zeta}\hat{\underline{\sigma}}' - {}_{n+\zeta}\hat{\underline{\sigma}}) + \frac{\text{T}\partial f_{vp}}{\partial \underline{X}_3} \Big|_{{}_{n+\zeta}\hat{\underline{\sigma}}, {}_{n+\zeta}\underline{X}_3} ({}_{n+\zeta}\underline{X}_3' - {}_{n+\zeta}\underline{X}_3) \right] \\ &\quad + (1 - 2\zeta) \left\| \underline{G}(\Delta \underline{E}' - \Delta \underline{E}) \right\|_G^2 \end{aligned} \quad (\text{A.12})$$

the integration of the convexity condition (Eq. (A.5)) following the mid-point rule, so:

$$\Delta t [f_{\text{vp}}(n+\varsigma \hat{\underline{\boldsymbol{\sigma}}}, n+\varsigma \underline{\boldsymbol{X}}_3) - f_{\text{vp}}(n+\varsigma \hat{\underline{\boldsymbol{\sigma}}}, n+\varsigma \underline{\boldsymbol{X}}_3)] \geq \Delta t \left[\frac{\text{T} \partial f_{\text{vp}}}{\partial \hat{\underline{\boldsymbol{\sigma}}}} \Big|_{n+\varsigma \hat{\underline{\boldsymbol{\sigma}}}, n+\varsigma \underline{\boldsymbol{X}}_3} (n+\varsigma \hat{\underline{\boldsymbol{\sigma}}} - n+\varsigma \hat{\underline{\boldsymbol{\sigma}}}) + \frac{\text{T} \partial f_{\text{vp}}}{\partial \underline{\boldsymbol{X}}_3} \Big|_{n+\varsigma \hat{\underline{\boldsymbol{\sigma}}}, n+\varsigma \underline{\boldsymbol{X}}_3} (n+\varsigma \underline{\boldsymbol{X}}_3 - n+\varsigma \underline{\boldsymbol{X}}_3) \right] \quad (\text{A.13})$$

leads to:

$$\|n_{+1} \underline{\boldsymbol{\Sigma}} - n_{+1} \underline{\boldsymbol{\Sigma}}\|_G^2 - \|n \underline{\boldsymbol{\Sigma}} - n \underline{\boldsymbol{\Sigma}}\|_G^2 \leq 2 \Delta t_{n+\varsigma} \dot{\lambda}_{\text{vp}} [f_{\text{vp}}(n+\varsigma \hat{\underline{\boldsymbol{\sigma}}}, n+\varsigma \underline{\boldsymbol{X}}_3) - f_{\text{vp}}(n+\varsigma \hat{\underline{\boldsymbol{\sigma}}}, n+\varsigma \underline{\boldsymbol{X}}_3)] + 2 \Delta t_{n+\varsigma} \dot{\lambda}_{\text{vp}} [f_{\text{vp}}(n+\varsigma \hat{\underline{\boldsymbol{\sigma}}}, n+\varsigma \underline{\boldsymbol{X}}_3) - f_{\text{vp}}(n+\varsigma \hat{\underline{\boldsymbol{\sigma}}}, n+\varsigma \underline{\boldsymbol{X}}_3)] + (1 - 2\varsigma) \left\| \underline{\underline{\boldsymbol{G}}}(\Delta \underline{\boldsymbol{\Xi}} - \Delta \underline{\boldsymbol{\Xi}}) \right\|_G^2 \quad (\text{A.14})$$

Now, using Eq. (67):

$$\|n_{+1} \underline{\boldsymbol{\Sigma}} - n_{+1} \underline{\boldsymbol{\Sigma}}\|_G^2 - \|n \underline{\boldsymbol{\Sigma}} - n \underline{\boldsymbol{\Sigma}}\|_G^2 \leq 2 \Delta t_{n+\varsigma} \dot{\lambda}_{\text{vp}} \left[f_{\text{vp}}^{\text{dyn}}(n+\varsigma \hat{\underline{\boldsymbol{\sigma}}}, n+\varsigma \underline{\boldsymbol{X}}_3; n+\varsigma \dot{\lambda}_{\text{vp}}) + \left(\frac{n+\varsigma \dot{\lambda}_{\text{vp}}}{K} \right)^{1/N} - f_{\text{vp}}^{\text{dyn}}(n+\varsigma \hat{\underline{\boldsymbol{\sigma}}}, n+\varsigma \underline{\boldsymbol{X}}_3; n+\varsigma \dot{\lambda}_{\text{vp}}) - \frac{n+\varsigma \dot{\lambda}_{\text{vp}}}{K} \right]^{1/N} + 2 \Delta t_{n+\varsigma} \dot{\lambda}_{\text{vp}} \left[f_{\text{vp}}(n+\varsigma \hat{\underline{\boldsymbol{\sigma}}}, n+\varsigma \underline{\boldsymbol{X}}_3; n+\varsigma \dot{\lambda}_{\text{vp}}) + \left(\frac{n+\varsigma \dot{\lambda}_{\text{vp}}}{K} \right)^{1/N} - f_{\text{vp}}(n+\varsigma \hat{\underline{\boldsymbol{\sigma}}}, n+\varsigma \underline{\boldsymbol{X}}_3; n+\varsigma \dot{\lambda}_{\text{vp}}) - \frac{n+\varsigma \dot{\lambda}_{\text{vp}}}{K} \right]^{1/N} + (1 - 2\varsigma) \left\| \underline{\underline{\boldsymbol{G}}}(\Delta \underline{\boldsymbol{\Xi}} - \Delta \underline{\boldsymbol{\Xi}}) \right\|_G^2 \quad (\text{A.15})$$

If the viscoplastic yield condition is enforced at the intermediate time $t_{n+\varsigma} \in [t_n, t_{n+1}]$:

$$\begin{aligned} f_{\text{vp}}^{\text{dyn}}(n+\varsigma \hat{\underline{\boldsymbol{\sigma}}}, n+\varsigma \underline{\boldsymbol{X}}_3; n+\varsigma \dot{\lambda}_{\text{vp}}) &\leq 0 & \text{if } f_{\text{vp}}(n+\varsigma \hat{\underline{\boldsymbol{\sigma}}}, n+\varsigma \underline{\boldsymbol{X}}_3) &\leq 0; & n+\varsigma \dot{\lambda}_{\text{vp}} &= 0 \\ f_{\text{vp}}^{\text{dyn}}(n+\varsigma \hat{\underline{\boldsymbol{\sigma}}}, n+\varsigma \underline{\boldsymbol{X}}_3; n+\varsigma \dot{\lambda}_{\text{vp}}) &= 0 & \text{if } f_{\text{vp}}(n+\varsigma \hat{\underline{\boldsymbol{\sigma}}}, n+\varsigma \underline{\boldsymbol{X}}_3) &> 0; & n+\varsigma \dot{\lambda}_{\text{vp}} &> 0 \end{aligned} \quad (\text{A.16})$$

this inequality becomes during a viscoplastic flow:

$$\|n_{+1} \underline{\boldsymbol{\Sigma}} - n_{+1} \underline{\boldsymbol{\Sigma}}\|_G^2 - \|n \underline{\boldsymbol{\Sigma}} - n \underline{\boldsymbol{\Sigma}}\|_G^2 \leq 2 \Delta t \left[\left(\frac{n+\varsigma \dot{\lambda}_{\text{vp}}}{K} \right)^{1/N} - \frac{n+\varsigma \dot{\lambda}_{\text{vp}}}{K} \right]^{1/N} (n+\varsigma \dot{\lambda}_{\text{vp}} - n+\varsigma \dot{\lambda}_{\text{vp}}) + (1 - 2\varsigma) \left\| \underline{\underline{\boldsymbol{G}}}(\Delta \underline{\boldsymbol{\Xi}} - \Delta \underline{\boldsymbol{\Xi}}) \right\|_G^2 \quad (\text{A.17})$$

$n+\varsigma \dot{\lambda}_{\text{vp}}$ and $n+\varsigma \dot{\lambda}_{\text{vp}}$ being positive, it comes finally that the generalised mid-point scheme applied to the considered viscoplastic constitutive equations is unconditionally B-stable for $\varsigma \geq 1/2$. For the generalised trapezoidal scheme, the B-stability remains an open problem.

Appendix B. Formulation of a time-dependent damage model

Considering the time-independent damaged elastic behaviour model defined in [1, Eq. (7)]:

$$\dot{\underline{\boldsymbol{\sigma}}} = \hat{\underline{\underline{\boldsymbol{S}}}}^{-1} \left(\dot{\underline{\boldsymbol{\varepsilon}}} - \dot{D} \frac{\partial f_d}{\partial \underline{\boldsymbol{\sigma}}} \right); \quad \hat{\underline{\underline{\boldsymbol{S}}}} = \underline{\underline{\boldsymbol{A}}}^{-1} + \underline{\underline{\boldsymbol{H}}}(D); \quad f_d = \frac{1}{2} \text{T} \underline{\underline{\boldsymbol{\sigma}}} \underline{\underline{\boldsymbol{H}}}' \underline{\underline{\boldsymbol{\sigma}}} - y(D); \quad \underline{\underline{\boldsymbol{H}}}' = \frac{\partial \underline{\underline{\boldsymbol{H}}}}{\partial D} \quad (\text{B.1})$$

with, from the consistency condition $\dot{f}_d = 0$:

$$\dot{D} = \frac{\text{T} \left(\frac{\partial f_d}{\partial \underline{\boldsymbol{\sigma}}} \right) \hat{\underline{\underline{\boldsymbol{S}}}}^{-1} \dot{\underline{\boldsymbol{\varepsilon}}}}{\text{T} \left(\frac{\partial f_d}{\partial \underline{\boldsymbol{\sigma}}} \right) \hat{\underline{\underline{\boldsymbol{S}}}}^{-1} \left(\frac{\partial f_d}{\partial \underline{\boldsymbol{\sigma}}} \right) - \text{T} \underline{\underline{\boldsymbol{\sigma}}} \underline{\underline{\boldsymbol{H}}}}'' \underline{\underline{\boldsymbol{\sigma}}} + y'}; \quad y' = \frac{\partial y}{\partial D}; \quad \underline{\underline{\boldsymbol{H}}}}'' = \frac{1}{2} \frac{\partial^2 \underline{\underline{\boldsymbol{H}}}}{\partial D^2} \quad (\text{B.2})$$

it comes:

$$\dot{\underline{\boldsymbol{\sigma}}} = \underline{\underline{\boldsymbol{B}}}^{\text{ed}} \dot{\underline{\boldsymbol{\varepsilon}}}; \quad \underline{\underline{\boldsymbol{B}}}^{\text{ed}} = \hat{\underline{\underline{\boldsymbol{S}}}}^{-1} - \frac{\hat{\underline{\underline{\boldsymbol{S}}}}^{-1} \frac{\partial f_d}{\partial \underline{\boldsymbol{\sigma}}} \text{T} \left(\hat{\underline{\underline{\boldsymbol{S}}}}^{-1} \frac{\partial f_d}{\partial \underline{\boldsymbol{\sigma}}} \right)}{\text{T} \left(\frac{\partial f_d}{\partial \underline{\boldsymbol{\sigma}}} \right) \hat{\underline{\underline{\boldsymbol{S}}}}^{-1} \left(\frac{\partial f_d}{\partial \underline{\boldsymbol{\sigma}}} \right) - \text{T} \underline{\underline{\boldsymbol{\sigma}}} \underline{\underline{\boldsymbol{H}}}}'' \underline{\underline{\boldsymbol{\sigma}}} + y'} \quad (\text{B.3})$$

The so constructed constitutive equations for the time-independent damage, where the strain rates $\dot{D} \partial f_d / \partial D$ arrive from the loss of stiffness, are closed to the classical plasticity ones including, for example, a stress softening which

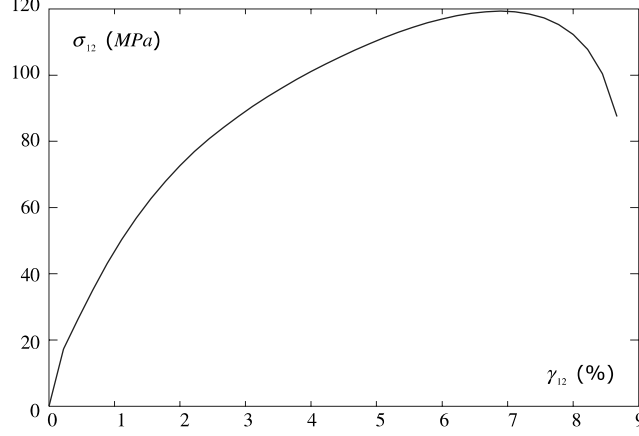


Fig. 12. Stress–strain curve of a damaged material by shearing-strain softening. The considered material is a single layer composite oriented along the loading direction: $E_1 = 60100$ MPa, $E_2 = 22350$ MPa, $G_{12} = 9300$ MPa, $Y_c = 0.0024$ MPa, $p = 0.61$ and $q = 0.41$.

induces a contraction of the elastic domain (see Fig. 12). Localisation under quasi-static loading conditions is then associated with a loss of ellipticity of the governing equations [35–37]. Standard boundary value problems become ill-posed and any numerical attempts to capture the solution will be meaningless since this solution is non-unique (strain rate jumps through singular surfaces) i.e. finite element computations exhibit spurious mesh sensitivity when the mesh is refined to vanishing size. These numerical difficulties may be overcome by viscous regularisation [38–40]. This technique retains the time-independent damage model characteristics and renders well-posed the considered boundary value problems.

In order to account for loading rate dependency and to regularise eventual localisation problems, a viscous damage mechanism is introduced in this appendix. Such a model accounts for retardation of the micro-cracks growth in the polymer matrix and then of the elastic module damage degradation.

Considering a linear Perzyna-type regularisation [41,42], the damage variable evolution equation governing a visco-damage behaviour is obtained from its time-independent counterpart [1] by replacing the Lagrange multiplier λ_d by $K_d \langle \dot{f}_d \rangle$, where $\langle \dot{f}_d \rangle = (f_d + |\dot{f}_d|)/2$, f_d being the damage yield function (Eq. (B.1)) i.e.

$$\dot{D} = K_d \langle \dot{f}_d \rangle \quad (\text{B.4})$$

By analogy with the viscoplastic behaviour (Section 2.2), the time-independent damage is recovered when $K_d \rightarrow \infty$.

A fully implicit integration (which leads to a first order accurate and B-stable algorithm) of this relation over the time interval $[t_n, t_{n+1}]$, gives:

$${}_{n+1}D = {}_nD + \Delta t K_d \langle \dot{f}_d({}_{n+1}\underline{\sigma}, {}_{n+1}D) \rangle; \quad {}_{n+1}\underline{\sigma} = \left[\underline{I} + \underline{A} \underline{H}({}_{n+1}D) \right]^{-1} {}_{n+1}\hat{\underline{\sigma}} \quad (\text{B.5})$$

This provides a non-linear equation $\bar{f}_d({}_{n+1}D) = 0$ to be solved using the Newton's method or any other suitable root finder in order to obtain the current damage variable ${}_{n+1}D$.

The key idea to evaluate an algorithmic tangent operator with a visco-damage model following the procedure adopted in [1], is to replace the damage consistency condition $df_d = 0$ by the analogous condition $d\bar{f}_d = 0$. Hence:

$$\underline{\underline{B}} = \left[\underline{\underline{L}} - \frac{\underline{L} \underline{A} \underline{H}' {}_{n+1}\underline{\sigma} ({}_{n+1}\underline{\sigma} {}_{n+1}\underline{H}' \underline{L})}{{}_{n+1}\underline{\sigma} (\underline{H}' \underline{L} \underline{A} \underline{H}' - \underline{H}'') {}_{n+1}\underline{\sigma} + y' + \left(\frac{1}{\Delta t K_d} \right)} \right] \hat{\underline{\underline{C}}}^{v,ep} \quad (\text{B.6})$$

Box 1: Constitutive frame of the viscoelastic equivalent virgin material

Stress-strain relationship:

$$\hat{\underline{\sigma}} = \underline{A} \hat{\underline{\varepsilon}}^c$$

$$\hat{\underline{\varepsilon}}^c = \underline{\varepsilon} - \hat{\underline{\varepsilon}}^{ve}(\underline{\xi}_i)$$

See Eq. (4) for \underline{A}

Evolution laws:

$$\dot{\hat{\underline{\varepsilon}}}^{ve} = \sum_i \dot{\underline{\xi}}_i$$

$$\dot{\underline{\xi}}_i = \frac{1}{\tau_i} (\mu_i \underline{S}_{ve} \hat{\underline{\sigma}} - \underline{\xi}_i)$$

See Eq. (5) for $\underline{S}_{ve} = \underline{A}^{-1}$

Incremental law:

$$\dot{\hat{\underline{\sigma}}} = \underline{A}(\dot{\underline{\varepsilon}} - \dot{\hat{\underline{\varepsilon}}}^{ve})$$

Relaxation times:

$$\tau_i = 10^{n_i}; \quad n_i = n_c - n_0 + (i - 1)\Delta; \quad \Delta = \frac{2n_0}{n_b - 1}$$

See (Fig. 1) for n_0 and n_c

Weighting coefficients:

$$\mu_i = + \frac{2}{n_0(n_b - 1)} [n_i - (n_c - n_0)] \quad \text{if } n_i \in [(n_c - n_0), n_c]$$

$$\mu_i = - \frac{2}{n_0(n_b - 1)} [n_i - (n_c + n_0)] \quad \text{if } n_i \in [n_c, (n_c + n_0)]$$

Box 2: Constitutive frame of the viscoplastic equivalent virgin material

Stress-strain relationship:

$$\hat{\underline{\sigma}} = \underline{A} \hat{\underline{\varepsilon}}^c$$

$$\hat{\underline{\varepsilon}}^c = \underline{\varepsilon} - \hat{\underline{\varepsilon}}^{vp}$$

“Dynamic” yield criterion:

$$f_{vp}^{dyn} = \overline{(\hat{\underline{\sigma}} - \underline{X}_3)} - \tau_0 - \left(\frac{\dot{\lambda}_{vp}}{K}\right)^{1/N} \leq 0$$

$$\overline{(\hat{\underline{\sigma}} - \underline{X}_3)} = \sqrt{T(\hat{\underline{\sigma}} - \underline{X}_3) \underline{M}(\hat{\underline{\sigma}} - \underline{X}_3)}$$

See Eq. (29) for \underline{M} . τ_0 is the initial threshold and $\dot{\lambda}_{vp}$ a viscoplastic multiplier

Evolution laws:

$$\dot{\hat{\underline{\varepsilon}}}^{vp} = \dot{\lambda}_{vp} \frac{\underline{M}(\hat{\underline{\sigma}} - \underline{X}_3)}{\overline{(\hat{\underline{\sigma}} - \underline{X}_3)}}$$

$$\dot{\underline{X}}_3 = \hat{\underline{\varepsilon}}^{vp}$$

Incremental laws:

$$\dot{\hat{\underline{\sigma}}} = \underline{A}(\dot{\underline{\varepsilon}} - \dot{\hat{\underline{\varepsilon}}}^{vp})$$

$$\dot{\underline{X}}_3 = \delta_3 \dot{\underline{X}}_3$$

Box 3: Instantaneous and time-dependent behaviours of the equivalent virgin material

Stress-strain relationship:
 $\hat{\underline{\sigma}} = \underline{A}\underline{\underline{\varepsilon}}^e$
 $\underline{\underline{\varepsilon}}^e = \underline{\varepsilon} - \underline{\varepsilon}^{ve} - \underline{\underline{\varepsilon}}^p - \underline{\underline{\varepsilon}}^{vp}$

Yield criteria:
 $f_p = \overline{(\hat{\underline{\sigma}} - \underline{X})} - \tau_0 \leq 0$
 $\overline{(\hat{\underline{\sigma}} - \underline{X})} = \sqrt{\text{T}(\hat{\underline{\sigma}} - \underline{X})\underline{M}(\hat{\underline{\sigma}} - \underline{X})}$; $\underline{X} = \underline{X}_1 + \underline{X}_2$
 $f_{vp}^{\text{dyn}} = f_{vp} - \left(\frac{\dot{\lambda}_{vp}}{K}\right)^{1/N} = \overline{(\hat{\underline{\sigma}} - \underline{X}_3)} - \tau_0 - \left(\frac{\dot{\lambda}_{vp}}{K}\right)^{1/N} \leq 0$
 See [1] for the plastic constitutive equations

Evolution laws:
 $\dot{\underline{\underline{\varepsilon}}}^{ve} = \sum_i \frac{1}{\tau_i} (\mu_i \underline{S}_{ve} \hat{\underline{\sigma}} - \underline{\underline{\varepsilon}}_i)$
 $\dot{\underline{\underline{\varepsilon}}}^p = \dot{\lambda}_p \frac{\underline{M}(\hat{\underline{\sigma}} - \underline{X})}{\overline{(\hat{\underline{\sigma}} - \underline{X})}}$
 $\dot{\underline{\underline{\varepsilon}}}^{vp} = \dot{\lambda}_{vp} \frac{\underline{M}(\hat{\underline{\sigma}} - \underline{X}_3)}{\overline{(\hat{\underline{\sigma}} - \underline{X}_3)}}$
 See box 1 for the relaxation times τ_i and the weighting coefficients μ_i

Incremental laws:
 $\dot{\hat{\underline{\sigma}}} = \underline{A}(\dot{\underline{\underline{\varepsilon}}} - \dot{\underline{\underline{\varepsilon}}}^{ve} - \dot{\underline{\underline{\varepsilon}}}^p - \dot{\underline{\underline{\varepsilon}}}^{vp})$
 $\dot{\underline{X}}_1 = \delta_1 \dot{\underline{\underline{\varepsilon}}}^p - \dot{\lambda}_p \gamma_1 \underline{M}\underline{X}_1$
 $\dot{\underline{X}}_2 = \delta_2 \dot{\underline{\underline{\varepsilon}}}^p$
 $\dot{\underline{X}}_3 = \delta_3 \dot{\underline{\underline{\varepsilon}}}^{vp}$

Box 4: Generalised trapezoidal scheme accuracy

(i) *Elastic prediction*
 Knowing the shear strain increment $\Delta\gamma_{12}$ and the state of the material at the end of the previous convergent increment (${}_n\hat{\underline{\sigma}}_{12}, {}_n(X_3)_{12}$), compute the elastic trial state:
 ${}_{n+1}\hat{\underline{\sigma}}_{12}^{\text{trial}} = {}_n\hat{\underline{\sigma}}_{12} + A_{44}\Delta\gamma_{12}$, ${}_{n+1}(X_3)_{12} = {}_n(X_3)_{12}$

Check the viscoplastic yield function:
 IF
 $f_{vp}[{}_{n+1}\hat{\underline{\sigma}}_{12}, {}_{n+1}(X_3)_{12}] = {}_{n+1}(\hat{\underline{\sigma}} - X_3)_{12} - \tau_0 < 0$
 the current step is elastic (${}_{n+1}\hat{\underline{\sigma}}_{12} = {}_{n+1}\hat{\underline{\sigma}}_{12}^{\text{trial}}$)

ELSE

(ii) *Viscoplastic correction*
 Compute:
 ${}_{n+1}\hat{\underline{\sigma}}_{12} = q^\zeta [{}_n\hat{\underline{\sigma}}_{12} + A_{44}\Delta\gamma_{12} - A_{44}\Delta t_n l(1 - \zeta)(1 - \delta_3 \Delta t_{n+1} l \zeta z^\zeta) {}_n(\hat{\underline{\sigma}} - X_3)_{12} + A_{44}\Delta t_{n+1} l \zeta z^\zeta {}_n(X_3)_{12}]$
 ${}_{n+1}(X_3)_{12} = z^\zeta [{}_n(X_3)_{12} + \delta_3 \Delta t_n l(1 - \zeta) {}_n(\hat{\underline{\sigma}} - X_3)_{12} + \delta_3 \Delta t_{n+1} l \zeta {}_{n+1}\hat{\underline{\sigma}}_{12}]$

with:
 $(q^\zeta)^{-1} = 1 + A_{44} \Delta t_{n+1} l \zeta v^\zeta$; $v^\zeta = 1 - \delta_3 \Delta t_{n+1} l \zeta z^\zeta$; $(z^\zeta)^{-1} = 1 + \delta_3 \Delta t_{n+1} l \zeta {}_{n+1}\hat{\underline{\sigma}}_{12} \frac{{}_{n+1}\dot{\lambda}_{vp}}{({}_{n+1}\dot{\lambda}_{vp}/K)^{1/N} + \tau_0}$

Compute the unknown ${}_{n+1}\dot{\lambda}_{vp}$ by solving:
 $\bar{f}_{vp}^{\text{dyn}}({}_{n+1}\dot{\lambda}_{vp}) = {}_{n+1}(\hat{\underline{\sigma}} - X_3)_{12} - \tau_0 - ({}_{n+1}\dot{\lambda}_{vp}/K)^{1/N} = 0$

(iii) *Relative error*
 Compute:
 $\frac{\text{Ref} \hat{\underline{\sigma}}_{12}(t_{n+1}) - {}_{n+1}\hat{\underline{\sigma}}_{12}}{\text{Re} \hat{\underline{\sigma}}_{12}(t_{n+1})} \quad \frac{\text{Ref} (X_3)_{12}(t_{n+1}) - {}_{n+1}(X_3)_{12}}{\text{Re} (X_3)_{12}(t_{n+1})}$

Box 5: Generalised mid-point scheme accuracy

(i) *Elastic prediction*

Knowing the shear strain increment $\Delta\gamma_{12}$ and the state of the material at the end of the previous convergent increment (${}_n\hat{\sigma}_{12}, {}_n(X_3)_{12}$), compute the elastic trial state:

$${}_{n+1}\hat{\sigma}_{12}^{\text{trial}} = {}_n\hat{\sigma}_{12} + A_{44}\Delta\gamma_{12}, \quad {}_{n+1}(X_3)_{12} = {}_n(X_3)_{12}$$

and:

$${}_{n+\zeta}\hat{\sigma}_{12}^{\text{trial}} = {}_n\hat{\sigma}_{12} + \zeta A_{44}\Delta\gamma_{12}, \quad {}_{n+\zeta}(X_3)_{12} = {}_n(X_3)_{12}$$

Check the viscoplastic yield function:

IF

$$f_{\text{vp}}[{}_{n+\zeta}\hat{\sigma}_{12}, {}_{n+\zeta}(X_3)_{12}] = {}_{n+\zeta}(\hat{\sigma} - X_3)_{12} - \tau_0 < 0$$

the current step is elastic (${}_{n+1}\hat{\sigma}_{12} = {}_{n+1}\hat{\sigma}_{12}^{\text{trial}}$)

ELSE

(ii) *Viscoplastic correction*

Compute:

$${}_{n+1}\hat{\sigma}_{12} = q^\zeta \{ {}_n\hat{\sigma}_{12} + A_{44}\Delta\gamma_{12} - A_{44}\Delta t_{n+\zeta} l [(1-\zeta)(1-\delta_3 \Delta t_{n+\zeta} l \zeta z^\zeta) {}_n(\hat{\sigma} - X_3)_{12} - \zeta z^\zeta ({}_n X_3)_{12}] \}$$

$${}_{n+1}(X_3)_{12} = z^\zeta \{ {}_n(X_3)_{12} + \delta_3 \Delta t_{n+\zeta} l [(1-\zeta) {}_n(\hat{\sigma} - X_3)_{12} + \zeta {}_{n+1}\hat{\sigma}_{12}] \}$$

with:

$$(q^\zeta)^{-1} = 1 + A_{44}\Delta t_{n+\zeta} l \zeta v^\zeta; \quad v^\zeta = 1 - \delta_3 \Delta t_{n+\zeta} l \zeta z^\zeta; \quad (z^\zeta)^{-1} = 1 + \delta_3 \Delta t_{n+\zeta} l \zeta_{n+\zeta} l \frac{{}_{n+\zeta}\dot{\lambda}_{\text{vp}}}{({}_{n+\zeta}\dot{\lambda}_{\text{vp}}/K)^{1/N} + \tau_0}$$

Compute the unknown ${}_{n+\zeta}\dot{\lambda}_{\text{vp}}$ by solving:

$$\bar{f}_{\text{vp}}^{\text{dyn}}({}_{n+\zeta}\dot{\lambda}_{\text{vp}}) = {}_{n+1}(\hat{\sigma} - X_3)_{12} - \tau_0 - ({}_{n+\zeta}\dot{\lambda}_{\text{vp}}/K)^{1/N} = 0$$

(iii) *Relative error*

Compute:

$$\frac{\text{Re} \hat{\sigma}_{12}(t_{n+1}) - {}_{n+1}\hat{\sigma}_{12}}{\text{Re} \hat{\sigma}_{12}(t_{n+1})} \quad \frac{\text{Re} (X_3)_{12}(t_{n+1}) - {}_{n+1}(X_3)_{12}}{\text{Re} (X_3)_{12}(t_{n+1})}$$

Box 6: Grid-search method associated with the classical Newton's iterative scheme

(i) Select an original square region in the positive $\Delta\lambda_{\text{p}}$ and ${}_{n+1}\dot{\lambda}_{\text{vp}}$ domain. This region is divided into m^2 squares, where the integer m is user determined.

(ii) Locate the squares having simultaneous zero-crossing curves of both functions \bar{f}_{p} and \bar{f}_{vp} within their boundaries.

(iii) Store the lower left corner co-ordinates ($\Delta\lambda_{\text{p}}^i, {}_{n+1}\dot{\lambda}_{\text{vp}}^i$) of the squares with simultaneous zero-crossing curves and their dimensions l_i in a stack.

(iv) Use the classical Newton's iterative scheme with the co-ordinates of the stored squares as starting values.

DO I = 1 TO SQUARENB

DO WHILE NEWTOL IS NOT SATISFIED

$$\begin{bmatrix} \partial \bar{f}_{\text{p}} / \partial \Delta\lambda_{\text{p}} & \partial \bar{f}_{\text{p}} / \partial {}_{n+1}\dot{\lambda}_{\text{vp}} \\ \partial \bar{f}_{\text{vp}} / \partial \Delta\lambda_{\text{p}} & \partial \bar{f}_{\text{vp}} / \partial {}_{n+1}\dot{\lambda}_{\text{vp}} \end{bmatrix}^i \begin{pmatrix} \delta \Delta\lambda_{\text{p}} \\ \delta {}_{n+1}\dot{\lambda}_{\text{vp}} \end{pmatrix}^i = - \begin{bmatrix} \bar{f}_{\text{p}}(\Delta\lambda_{\text{p}}^i, {}_{n+1}\dot{\lambda}_{\text{vp}}^i) \\ \bar{f}_{\text{vp}}(\Delta\lambda_{\text{p}}^i, {}_{n+1}\dot{\lambda}_{\text{vp}}^i) \end{bmatrix}, \quad \begin{pmatrix} \Delta\lambda_{\text{p}}^{i+1} \\ {}_{n+1}\dot{\lambda}_{\text{vp}}^{i+1} \end{pmatrix} = \begin{pmatrix} \Delta\lambda_{\text{p}}^i \\ {}_{n+1}\dot{\lambda}_{\text{vp}}^i \end{pmatrix} + \begin{pmatrix} \delta \Delta\lambda_{\text{p}} \\ \delta {}_{n+1}\dot{\lambda}_{\text{vp}} \end{pmatrix}^i$$

IF $\Delta\lambda_{\text{p}}^{i+1} < 0$ OR ${}_{n+1}\dot{\lambda}_{\text{vp}}^{i+1} < 0$ GO TO THE NEXT SQUARE

END DO

IF CONVERGENCE, GO OUT

END DO

(v) If the dimension of the square at the top of the stack is greater than the desired precision ε , where ε is user determined, take it from the stack, set the number of grid divisions m to 2 and go to (ii) to refine the search.

(vi) If the dimension of the square at the top of the stack is less than or equal to the desired precision, take it from the stack and go to (v).

Box 7: Multi-step predictor–corrector scheme

- (i) *Elastic–viscoelastic prediction in the effective stress space*
 Knowing the total strain increment $\Delta \underline{\epsilon}$ and the state of the material at the previous convergent increment $({}_n \hat{\underline{\sigma}}, {}_n \underline{\xi}, {}_n \underline{X}_1, {}_n \underline{X}_2, {}_n \underline{X}_3)$ compute the trial stresses ${}_{n+1} \hat{\underline{\sigma}}^{\text{trial}}$
 Check the plastic yield function:
 IF $f_p({}_{n+1} \hat{\underline{\sigma}}^{\text{trial}}, {}_n \underline{X}_1, {}_n \underline{X}_2) < 0$
 Check the viscoplastic yield function:
 IF $f_{vp}({}_{n+1} \hat{\underline{\sigma}}^{\text{trial}}, {}_n \underline{X}_3) < 0$; ${}_{n+\zeta} \hat{\underline{\sigma}}^{\text{trial}} = (1 - \zeta) {}_n \hat{\underline{\sigma}} + \zeta {}_{n+1} \hat{\underline{\sigma}}^{\text{trial}}$
 the current step is elastic (${}_{n+1} \hat{\underline{\sigma}} = {}_{n+1} \hat{\underline{\sigma}}^{\text{trial}}$)
 ELSE
 Viscoplastic correction:
 Compute ${}_{n+1} \hat{\underline{\sigma}}, {}_{n+1} \underline{X}_3$
 the viscoplastic multiplier ${}_{n+\zeta} \dot{\lambda}_{vp}$ is obtained by solving $\bar{f}_{vp}^{\text{dyn}}({}_{n+\zeta} \dot{\lambda}_{vp}) = 0$
 END IF
 ELSE
 Check the viscoplastic yield function:
 IF $f_{vp}({}_{n+\zeta} \hat{\underline{\sigma}}^{\text{trial}}, {}_n \underline{X}_3) < 0$
 Plastic correction
 Compute ${}_{n+1} \hat{\underline{\sigma}}, {}_{n+1} \underline{X}_1, {}_{n+1} \underline{X}_2$
 the plastic multiplier increment $\Delta \lambda_p$ is obtained by solving $\bar{f}_p(\Delta \lambda_p) = 0$
 ELSE
 Plastic and viscoplastic correction
 Compute ${}_{n+1} \hat{\underline{\sigma}}, {}_{n+1} \underline{X}_1, {}_{n+1} \underline{X}_2, {}_{n+1} \underline{X}_3$
 the multipliers $\Delta \lambda_p$ and ${}_{n+\zeta} \dot{\lambda}_{vp}$ are obtained by solving $\begin{cases} \bar{f}_p(\Delta \lambda_p) = 0 \\ \bar{f}_{vp}^{\text{dyn}}({}_{n+\zeta} \dot{\lambda}_{vp}) = 0 \end{cases}$
 END IF
 END IF
- (ii) *Elastic–viscoelastic–plastic–viscoplastic prediction in the true stresses space*
 Knowing the damage variable ${}_n D$ at the end of the previous convergent increment compute the trial stresses:
 ${}_{n+1} \underline{\sigma}^{\text{trial}} = \underline{L}_{n+1} \hat{\underline{\sigma}}; \quad \underline{L}^{-1} = \underline{I} + \underline{AH}({}_n D)$
 Check the damage yield function:
 IF $f_d({}_{n+1} \underline{\sigma}^{\text{trial}}, {}_n D) < 0$
 the current step is such as ${}_{n+1} \underline{\sigma} = {}_{n+1} \underline{\sigma}^{\text{trial}}$
 ELSE
 Damage correction
 Compute the final stresses and damage variable:
 ${}_{n+1} \underline{\sigma} = \underline{L}_{n+1} \hat{\underline{\sigma}}; \quad \underline{L}^{-1} = \underline{I} + \underline{AH}({}_{n+1} D)$
 ${}_{n+1} D$ is obtained by solving $f_d({}_{n+1} \underline{\sigma}, {}_{n+1} D) = 0$
 END IF

References

- [1] Boubakar ML, Trivauday F, Perreux D, Vang L. A meso–macro finite element modelling of laminate structures. Part I: Time-independent behaviour. *Compos Struct* 2002;58(2):271–86.
- [2] Germain P. *Cours de Mécanique des Milieux Continus; Tome 1*. Paris: Masson et Cie; 1971.
- [3] Halphen B, Nguyen QS. Sur les matériaux standards généralisés. *J Mécanique* 1975;14(1):39–63.
- [4] Germain P, Nguyen QS, Suquet P. Continuum thermodynamics. *J Appl Mech* 1983;50:1010–20.
- [5] Nowick AS, Berry BS. *Anelastic relaxation in crystalline solids*. New York: Academic Press; 1972.
- [6] Maire JF. *Etudes théorique et expérimentale du comportement de matériaux composites en contraintes planes*. PhD thesis of Franche-Comté University, No. 282, 1992.
- [7] Lemaitre J, Chaboche JL. *Mécanique des matériaux solides*. Paris: Dunod; 1988.
- [8] Rockafellar RT. *Convex analysis*. Princeton, NJ: Princeton University Press; 1972.
- [9] Duvaut G, Lions JL. *Inequalities in mechanics and physics*. Berlin: Springer; 1972.
- [10] Peric D. On a class of constitutive equations in viscoplasticity: Formulation and computational issues. *Int J Numer Meth Engng* 1993;36:1365–93.

- [11] Ibrahimbegovic A, Gharzeddine F, Chorfi L. Classical plasticity and viscoplasticity models reformulated: Theoretical basis and numerical implementation. *Int J Numer Meth Engng* 1998;42:1499–535.
- [12] Alfano G, De Angelis F, Angelis L. General solution procedures in elasto/viscoplasticity. *Comput Meth Appl Mech Engng* 2001;190:5123–47.
- [13] Vang L, Boubakar ML, Trivaudey F, Perreux D. Coupled damaged elasto-dissipative models for numerical analysis of shell composites. *I.C.C.M.* vol. 13, Beijing, China, June 25–29, 2001.
- [14] Ponthot JP. Radial return extensions for visco-plasticity and lubricated friction. In: *International Conference on Structural Mechanics and Reactor Technology SMIRT-13*, vol. 2, Porto Alegre, Brazil, 1995. p. 711–22.
- [15] Carosio A, William K, Etse G. On the consistency of viscoplastic formulations. *Int J Solids Struct* 2000;37:7349–69.
- [16] Ortiz M, Popov EP. Accuracy and stability of integration algorithms for elastoplastic constitutive equations. *Int J Numer Meth Engng* 1985;21:1561–76.
- [17] Butcher JC. A stability property of implicit Runge–Kutta methods. *BIT* 1975;15:358–61.
- [18] Burrage K, Butcher JC. Stability criteria for implicit Runge–Kutta methods. *SIAM J Numer Math* 1979;16:46–57.
- [19] Burrage K, Butcher JC. Non-linear stability of a general class of differential equation methods. *BIT* 1980;20:185–203.
- [20] Simo JC, Govindjee S. Non-linear B-stability and symmetry preserving return mapping algorithms for plasticity and viscoplasticity. *Int J Numer Meth Engng* 1991;31:151–76.
- [21] Simo JC. Non-linear stability of the time-discrete variational problem of evolution in non-linear heat conduction, plasticity and viscoplasticity. *Comput Meth Appl Mech Engng* 1991;88:111–31.
- [22] Simo JC, Ju JW. Strain and stress-based continuum damage models. II. Computational aspects. *Int J Solids Struct* 1987;23(7):841–69.
- [23] Ju JW. On energy-based coupled elastoplastic damage theories: Constitutive modeling and computational aspects. *Int J Solids Struct* 1989;25(7):803–33.
- [24] Ikonomopoulos G, Boubakar ML, Perreux D. Elastoplastic damaged finite element model for composite shells. In: *IASS—IACM 2000, Fourth International Colloquium on Computations of Shell & Spatial Structures*, Chania, Crete, Greece, 2000.
- [25] Lee J, Fenves GL. A return-mapping algorithm for plastic-damage models: 3-D and plane stress formulation. *Int J Numer Meth Engng* 2001;50:487–506.
- [26] Criesfield MA. In: *Non-linear finite element analysis of solids and structures*, vol. 1. Wiley: New York; 1997.
- [27] Dennis Jr JE, Schnabel RB. Numerical methods for unconstrained optimization and nonlinear equations. *Classics Appl Math*, SIAM 1996.
- [28] Richard F. Identification du comportement et évaluation de la fiabilité des composites stratifiés. PhD Thesis of Franche-Comté University, No. 769, France, 1999.
- [29] Hostetter GH, Santana M, D’Carpio-Montalvo P. Analytical, numerical and computational methods for science and engineering. Englewood Cliffs, NJ: Prentice Hall; 1991.
- [30] Nagtegaal JC. On the implementation of inelastic constitutive equations with special reference to large deformation problems. *Comput Meth Appl Mech Engng* 1982;33:469–84.
- [31] Simo JC, Taylor RL. Consistent tangent operators for rate-independent elastoplasticity. *Comput Meth Appl Mech Engng* 1985;48:101–18.
- [32] Simo JC, Taylor RL. A return mapping algorithm for plane stress elastoplasticity. *Int J Numer Meth Engng* 1986;22:649–70.
- [33] Cescotto S, Charlier R. Numerical simulation of elastic-visco-plastic large strains of metal at high temperature. in: *Proceedings of the International Conference of Structural Mechanics in Reactor Technology*, Brussels, 1985.
- [34] Kojic M, Bathe KJ. The effective-stress-function algorithm for thermo-elasto-plasticity and creep. *Int J Numer Meth Engng* 1987;24:1509–32.
- [35] Zhu YY, Cescotto S. A fully coupled elasto-visco-plastic damage theory for anisotropic materials. *Int J Solids Struct* 1995;32(11):1607–41.
- [36] Needleman A. Material rate dependence and mesh sensitivity in localisation problems. *Comput Meth Appl Mech Engng* 1988;67:69–85.
- [37] Loret B, Prevost JH. Dynamic strain localization in elasto-(visco)plastic solids. Part 1. General formulation and one dimensional examples. *Comput Meth Appl Mech Engng* 1990;83:247–73.
- [38] Prevost JH, Loret B. Dynamic strain localization in elasto. Plane strain exemples. *Comput Meth Appl Mech Engng* 1990;83:275–94.
- [39] Ju JW. On energy-based coupled elastoplastic damage theories: constitutive modelling and computational aspects. *Int J Solids Struct* 1989;25(7):803–33.
- [40] Benallal A, Billardon R, Lemaitre J. Continuum damage mechanics and local approach to fracture: numerical procedures. *Comput Meth Appl Mech Engng* 1991;92:141–55.
- [41] Govindjee S, Kay GJ, Simo JC. Anisotropic modelling and numerical simulation of brittle damage in concrete. *Int J Numer Meth Engng* 1995;38:3611–33.
- [42] Perzyna P. Fundamental problems in viscoplasticity. In: *Advances in applied Mechanics*, vol. 9. New York: Academic Press; 1966. p. 244–368.